THE IMPLEMENTATION OF A PORE PRESSURE AND FRACTURE GRADIENT PREDICTION MODEL FOR THE NORTH SEA CENTRAL JUDY AND JADE FIELDS

By

JAGADEESH KILAPARTHI

August 2013

Coventry University

A report submitted to the Department of Geography, Environment and Society, Coventry University in partial fulfilment of the requirements for a MSc in Petroleum and Environmental Technology

ABSTRACT

The purpose of this project is to implement a pore pressure and fracture gradient prediction strategy for the North Sea Central (Judy and Jade) fields. Measured porosity and pressure data of Judy and Jade fields will be studied and reviewed. This strategy will help to safe drilling, design and completion operations for future wells in these areas.

Judy and Jade field's data will examine and review on two pore pressure prediction models and one fracture gradient prediction model.

The pore pressure prediction from porosity model was examined primarily in this project to predict the pore pressure and pore pressure gradient. This was new theoretical model of pore pressure prediction, utilizes porosity to predicting the pore pressure. The pore pressure prediction from porosity model allowing normal compaction trendline of porosity to predict the pore pressure.

The Tau model was examined secondarily in this project to predict the pore pressure and pore pressure gradient. This model was derived based on interval velocity and transit time data. Tau model was proposed by Shell, this method dependent on velocity to predict the pore pressure.

In this project, the fracture pressure and fracture gradient prediction was done based on Kirsch's solution. The data required for this prediction strategy is overburden stress of formation, pore pressure and Poisson's ratio. Generally, minimum stress method and tensile failure methods were used in drilling industry. Kirsch's solution comes under tensile failure method, this prediction strategy delivered simple and accurate results to estimate the fracture pressure gradient.

The two pore pressure prediction strategies examined on available data, that two model pore pressure gradient results compared with the available pore pressure gradient data. Ultimately, Tau model based pore pressure prediction strategy delivered best results. Thus, the Tau model based pore pressure prediction strategy was preferred for future operations in Judy and Jade fields.

RESEARCH DECLARATION

I declare that this dissertation is completely my own work and any use of the others work has been properly acknowledged. I also confirm that this project has been conducted in accordance with the University's ethics guide.

I agree that the research work can be made available as a Reference Document to other students in the Department of Geography, Environment and Disaster Management.

Signed: ……………………………..   Date: …………………………………

Author's Name*:* JAGADEESH KILAPARTHI

ACKNOWLEGEMENTS

TABLE OF CONTENTS   **page numbers**

LIST OF TABLES

TABLE OF FIGURES

LIST OF PLOTS

NOMENCLATURE

p_f = the formation fluid pressure (psi);

σ_V = overburden stress (psi);

α_V = the normal overburden stress gradient (psi/ft);

β = the normal fluid pressure gradient (psi/ft);

Z = the depth below the mudline or below sea surface (ft);

t = the sonic transit time (μs/ft);

A, B = the constants;

P_{pg} = the formation pore pressure gradient;

OBG = the overburden stress gradient;

P_{ng} = the hydrostatic pore pressure gradient (normally 0.45 psi/ft or 1.03 MPa/km, dependent on water salinity);

R = the shale resistivity obtained from well logging;

R_n = the shale resistivity at the normal (hydrostatic) pressure;

n = the exponent varied from 0.6 to 1.5, and normally n =1.2;

t_n = the sonic transit time or slowness in shales at the normal pressure;

t = the sonic transit time in shales obtained from well logging;

v_p = the compressional velocity at a given depth;

v_{ml} = the compressional velocity in the mudline;

t_{ml} = the compressional transit time in the mudline;

U = the uplift parameter

σ_{max} and v_{max} = the estimates of the effective stress and velocity at the onset unloading.

p_{ulo} = the pore pressure in the unloading case;

v_m = the sonic interval velocity in the matrix of the shale;

v_p = the compressional velocity at a given depth;

λ = the empirical parameter;

d_{max} = the depth at which the unloading has occurred;

A_s ,B_s = the fitting constants;

The best fitting parameters in the Gulf of Mexico are A_s = 1989.6 and B_s = 0.904 (Gutierrez et al, 2006), (for Judy and Jade fields A_s = 1391.5 and B_s = 0.302 are assumed);

τ = the Tau variable;

C = the constant related to the mudline transit time (normally C = 200 μs/ft);

D = the constant related to the matrix transit time (normally D = 50 μs/ft);

Δt = the compressional transit time (70 μs/ft);

R_n = the shale resistivity in the normal compaction condition;

R_0 = the shale resistivity in the mudline;

b = the constant;

Z = the depth below the mudline;

R = the measured shale resistivity at depth of Z;

R_0 = the normal compaction shale resistivity in the mudline;

b = the slope of logarithmic resistivity normal compaction trendline;

v = the seismic velocity at depth of Z;

v_0 = the velocity in the ground surface or at the sea floor;

k = a constant;

t_n = the acoustic transit time (μs/m);

t_m = the compressional transit time in the shale matrix (with zero porosity);

t_{ml} = the mudline transit time;

c = the constant;

φ = porosity;

φ_0 = the porosity in the mudline;

Z = the true vertical depth below the mudline;

c = the compaction constant in 1/m or 1/ft.

a = the stress compaction constant in 1/psi or 1/MPa;

C_m = the constant related to the compressional transit time in the matrix and the transit time in the mudline;

Δt_f = the transit time of interstitial fluids;

σ_{min} = the minimum in-situ stress or the lower bound of fracture pressure;

v = the Poisson's Ratio;

P_{FG} is the formation fracture gradient;

P_{pg} = the formation pore pressure gradient;

OBG = the overburden stress gradient;

K_0 = the effective stress coefficient;

σ_V' = the maximum effective in-situ stress or effective overburden stress;

P_{FPmax} = the upper bound of fracture pressure;

σ_H = the maximum horizontal stress;

σ_{min} = the minimum horizontal stress or minimum in-situ stress;

σ_T = the thermal stress induced by the difference between the mud temperature and the formation temperature;

T_0 = the tensile strength of the rock;

P_{FP} = the fracture pressure.

Ftbsf = feet below sea floor.

CHAPTER 1

1.0 INTRODUCTION

1.1 BACKGROUND

Pore pressure and fracture pressure gradients determinations are vital considerations for the successful planning and drilling of North Sea Central Graben High Pressure High Temperature (HPHT) wells. Understanding of these downhole pressure limitations can have a substantial effect on drilling safety and economics. An exact estimate of the sub-surface pore pressures and fracture gradients is a crucial constraint to safely, economically and efficiently drill the wells required to test and produce oil and natural gas reserves. Pore pressures are simply predicted for normally pressure sediments. It is the prediction of pore pressures for the abnormally pressured (i.e. over pressured) sediments that is more difficult and more important. An understanding of the pore pressure is a requirement of the drilling plan in order to choose proper casing points and design a casing program that will allow the well to be drilled most effectively and maintain well control during drilling and completion operations. Well control events such as formation fluid kicks, lost circulation, surface blowouts and underground blowouts can be avoided with the use of accurate pore pressure and fracture gradient predictions in the design process (Fooshee, S. 2009).

The pressure regime of the Central Graben in the North Sea presents a formidable challenge for both exploration drilling and field development. In this area, we apply a practical approach to improve pore-pressure and fracture pressure prediction from seismic velocities derived from amplitude variation with offset (AVO) information. The emphasis is placed on maximising both temporal and lateral resolution of the pressure estimates. Besides assisting exploration well planning, improved resolution may define local pressure variations around a reservoir that assists field appraisal and development. Pressure data from one well in the area is used to calibrate the pressure predictions from seismic velocities and to refine the parameters controlling the predictions. The refined laterally invariant parameters are applied to seismic velocities derived from non- proprietary data over an approximate 500 km2 area in the Central Graben (Hawkins, K. 2004).

The variable pressure regime of the Central Graben in the North Sea presents a number of challenges. There are the deep high pressure – high temperature (HPHT) Jurassic and Triassic reservoirs, which are among the most overpressured in the world. Shallower, are the moderately overpressured porous Cretaceous Chalk reservoirs. They are encased in impermeable chalk that prevents accurate pressure measurement or prediction. Above the Chalk are Paleocene reservoirs, which although more normally pressured, exist beneath an overpressured younger Tertiary section. All of these reservoirs require careful adjustment of mud weight: (a) to avoid dangerous blowouts in the HPHT environment, (b) to avoid surprise kicks within the Chalk formations and (c) to limit mud invasion into the Paleocene and some Chalk reservoirs that could hinder appraisal, or even prevent discovery. High pressure – high temperature (HPHT) reservoirs are increasingly becoming the focus of petroleum exploration in the search for additional reserves. The processes leading to the accumulation and preservation of hydrocarbons in these extreme settings are still poorly constrained, especially also with respect to the occurrence of significant porosity at temperatures exceeding 150°C and pressures approaching lithostatic. The processes controlling the evolution of fluid pressure during reservoir burial have been studied by various authors. Overpressure generating mechanisms have been reviewed by Osborne and

Swarbrick (1997), who postulated that disequilibrium compaction is the main mechanism controlling overpressure in the Central Graben. This opinion is supported also by Mann and Mackenzie (1990), although the importance of additional overpressure generation due to gas generation is becoming increasingly acknowledged (Cayley, 1986; Isaksen, 2004; Swarbrick, et al. 2000).

1.2 Aim:
The aim of this project to improve the knowledge and verification of pore pressure and fracture gradient prediction models for Judy and Jade fields in North Sea Central HPHT Wells.

1.3 Objectives:
The main objectives of this project are:
(1) To understanding pore pressure prediction in unconventional plays, is important for executing a safe drilling strategy and for accurate production modelling.
(2) To clear understanding of the petro physical data.
(3) To review of pore pressure prediction models.
(4) To verify and determine suitable pore pressure and fracture gradient model for Judy and Jade fields in North Sea Central HPHT Wells.

The purpose of this project is to develop a pore pressure and fracture gradient prediction strategy for the North Sea central HPHT wells, namely the Jade and Judy fields in Quadrant 30, UK North Sea, using petro physical and measured pressure data for wells previously drilled in North Sea central HPHT wells area will be examined and reviewed. The pore pressure and fracture gradient prediction strategy will be useful when designing future drilling and completion operations in the aforementioned area.

CHAPTER 2
2. 0 LITERATURE REVIEW

Prediction of Pore-pressure depends greatly on understanding of seismic and well characteristics for instance velocity, resistivity, and density which capture porosity changes during shale compaction under vertical loading. Relationships were developed by Eaton (1975) in the Gulf of Mexico using a moderately simple lithological mix of geologically young sandstones and shale mud rocks at moderately low temperatures. An alternative method using data from the same region was more deterministic—also with vertical stress (e.g., Hottman and Johnson, 1965; Bowers, 1995). Another method using mean stress, developed by Harrold et al. (2000) used comparable sand and shale structures at moderately low temperatures from data in Southeast Asia basins. All the above methodologies can be shown to deliver satisfactory estimate of pore pressure in shale mud rocks in young, quickly placed siliciclastic arrangements, for instance the Baram Delta, Brunei (Tingay et al. 2009) and laterally the West African margin (Swarbrick et al. 2011). The results can be standardised, through cautious consideration to indication for adjacent drainage or adjacent transfer, by means of data from their related reservoir. Though, in higher-temperature environments (e.g., Malay Basin, Hoesni 2004) these approaches be unsuccessful to convey estimates which could be precise sufficient for actual well planning and safe drilling.

The foremost determination of this literature review was accomplished to improvement understanding of diverse pore pressure and fracture gradient estimate approaches in an exertion to find the finest approach for this area. This review, though, is not fully thorough by means of there are a massive numeral of approaches that have been established meanwhile the middle of the twentieth century. This review is inadequate to a limited pore pressure estimate approaches and two fracture gradient estimate approaches. However realising the several pore pressure and fracture gradient estimate approaches, a determination was made to validate or conclude the petro physical data essential for a comprehensive estimate approach. Those approaches will also be comprised in the literature review.

2.1 PORE PRESSURE AND FRACTURE PRESSURE PREDICTION STRATEGIES

Overpressures can be made through various mechanism, for instance compaction imbalance means Undercompaction, generation of hydrocarbons, cracking process of gas, aqua thermal expansion, lateral stress in formations, transformation of minerals (i.e., illitiza-tion), and process of osmosis, hydrostatic column and resistance of hydrocarbons (Swarbrick and Osborne, 1998; Gutierrez et al. 2006). In all cases where compaction disequilibrium has been calculated to be the main reason of over pressuring, the time of life of the rocks is geologically young. Instances of regions where compaction disequilibrium is named as the crucial cause of abnormal pressure include the U.S. Gulf Coast, Alaska Cook Inlet, Beaufort Sea, Mackenzie Delta, North Sea, Adriatic Sea, Niger Delta, Mahakam Delta, the Nile Delta, Malay Basin, Eastern Venezuelan Basin (Trinidad) and the Pot war Plateau of Pakistan (Powley, 1990; Burrus, 1998; Heppard et al. 1998; Law and Spencer, 1998; Nelson & Bird 2005; Morley et al. 2011). In these regions, the unusually pressured rocks are mostly situated in Tertiary and late Mesozoic sedimentary formations, the depositional setting is dominantly deltaic, and the lithology is dominantly shale.

Abnormal formation compaction such as compaction disequilibrium, Undercompaction are main causes for abnormal pore pressure. Pore fluid eviction and compression of formation porosity occurred generally where deposits compressed. The foremost cause of fluid barring is overburden pressure increasing with depth. The rate of sedimentation and normal compaction are vice versa, means if normal compaction rises, the rate of sedimentation is becoming slow. Fluids expel ability effects the equilibrium between overburden rise and volume of pore fluid reduction (Mouchet & Mitchell 1989). The hydrostatic pore pressure generation depends on the normal compaction. Though, quick burial hints to quicker exclusion of fluids in answer to quickly growing overburden stress. At what time the deposits recede quickly, or else the formation has enormously little permeability, fluids in the deposits can only be incompletely ejected. That continued fluid in the pores of the deposits essential backing them or portion of the heaviness of excessively deposits, producing the pressure of pore fluid rises, unusually great pore pressure.

Two pore pressure prediction strategies and one fracture gradient prediction strategy will be reviewed and applied to the available data. The two pore pressure prediction strategies require petro physical data, specifically formation resistivity or conductivity, to predict pore pressures. The fracture gradient prediction strategy requires an accurate estimate of pore Pressure.

The first pore pressure prediction strategy reviewed was developed by seismic velocity pore pressure prediction model. This strategy utilizes a series of geologic age specific overlays, which indicate the normally pressured compaction trend lines for the respective geologic age. After plotting the observed resistivity/conductivity data on the geologic age specific overlay, the pore pressures can be predicted. A simple calibration of the data was required to establish the normal pressure trend line implemented in this method.

The second pore pressure prediction strategy reviewed was developed by Ben Eaton (1975). Eaton developed a simple relationship that will predict the pore pressure knowing the normally pressured compaction trend line, the observed resistivity/conductivity data and a relationship for the overburden stress versus depth. The fracture pressure prediction strategy reviewed was also developed by Ben Eaton (1975). The data required for this prediction strategy is formation overburden stress, pore pressure and Poisson's ratio of the formation. A relationship for the overburden stress and Poisson's ratio can be developed based on field data, or one of Eaton's generalized relationships can be used.

2.2 PORE PRESSURE AND PORE PRESSURE GRADIENT

Estimation of Pore pressure plays key role in the planning of well drilling and for geomechanical, geological analysis. Pore pressure means the fluids exerted pressures in the pore spaces in porous formations. Some types of Pore pressures are hydrostatic pressure, abnormal pressure and overburden pressure, it be changes from hydrostatic pressure, to over burden pressure (48% to 95% of the overburden stress). Hydrostatic pressure is normally called normal pressure, if the pore pressure is lesser or upper than the hydrostatic pressure (normal pore pressure), it is called abnormal pore pressure and when pore pressure more than hydrostatic pressure (normal pore pressure), it is called overburden pressure.

Pore pressure prediction's basic theory derived from Terzaghi's and Biot's effective stress law (Biot. 1941; Terzaghi et al. 1996). This fundamental theory represents the formation pore pressure is a function of overburden stress and effective stress. The Terzaghi's and Biot's effective stress law generated a correlation to explain the relationship of overburden stress, effective vertical stress and pore pressure. It can be expressed in the following form:

$$p = (\sigma_V - \sigma_e) / \alpha \qquad\qquad (1)$$

Where pore pressure (p); overburden stress (σ_V); vertical effective stress (σ_e); and Biot effective stress coefficient (α). It is usually assumed $\alpha=1$ in geo pressure community.

Pore pressure calculation from equation (1) depends on overburden stress and effective stress. When these two stresses known, can be calculated pore pressure. Bulk density logs and well log data, for instance resistivity, sonic travel time/ velocity, bulk density and drilling parameters (e.g., D exponent) generally used to generate the data of overburden stress, effective stress. The hydrostatic pressure, vertical effective stress, overburden stress and formation pore pressure profiles demonstrated with the true vertical depth (TVD) in Fig. 1 of a characteristic oil and gas exploration well. The pore pressure trend line with true vertical depth in these fields are comparable to several sedimentary young fields where over pore pressure is come across at depth. Pore pressure is hydrostatic, that indicating continuous unified column of formation pore fluid spreads from surface to depth at moderately low depths (less than 2000 m). At more than 2000 m depths, pore pressure increases with true vertical depth quickly and overpressure is started, This represents the deeper formations hydraulically remote from shallower formations. If pore pressure value reaches by 3800 m near to the overburden stress value, that state mentioned as hard overpressure. The subtraction value of pore pressure (p) from overburden stress (σ_V) conventionally defined as effective stress (σ_e) as shown in Fig. 1. The overpressure increase represents the reduction of the effective stress.
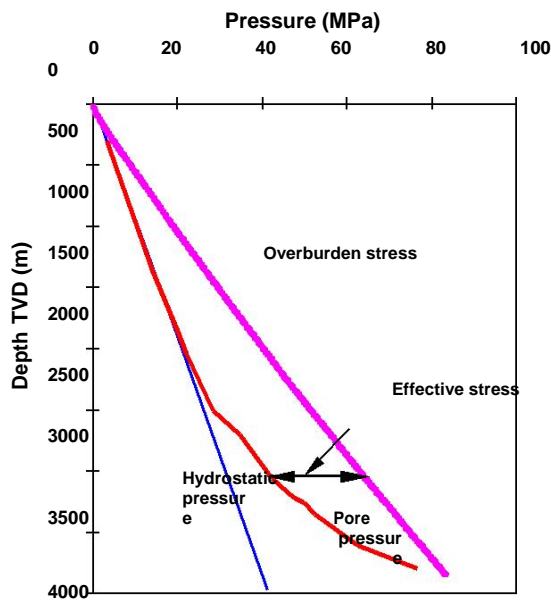
Figure 1. Hydrostatic pressure, pore pressure, overburden stress, and effective stress in a borehole (Zhang 2011: 52).

In drilling engineering, pore pressure gradient is one of the vital parameter, it is basically used to determining the mud weight (or mud density) and practically pore pressure gradient more convenient to use for safe drilling as shown in Fig. 2. At a given true vertical depth, the pore pressure gradient can be determined as the pore pressure divided by the true vertical depth. The main purpose of pore pressure gradient and fracture gradient is used to appropriate selection of mud weight, wellbore stability, setting and cementing a casing. Wellbore collapse and prevention of influx in wellbore are major problems during drilling, for the reason that the drilling fluid (mud) is acts as mud pressure. Mud pressure should be heavier than pore pressure to avoid and prevent kicks, wellbore instability and fluid influx in an open hole section during drilling. Conversely, mud weights should be lower than the fracture gradient, otherwise it causing to fracturing the formation, lost circulation and mud losses.

The analysis of pore pressure mainly having three parts: (a) Pre-drill pore pressure prediction analysis. (b) Pore pressure prediction while drilling analysis. (c) Post-well pore pressure analysis. In the pre-drill pore pressure analysis, seismic interval velocity data used for the planned wells to predicting the pre-drill pore pressure as well as for the offset wells well logging and drilling data used to predicting the pre-drill pore pressure. In the pore pressure prediction while drilling analysis, the logging while drilling (LWD), drilling parameters, mud logging data and measurement while drilling (MWD) are mainly used to analyse pore pressures. In The post-well analysis, all available data used to construct pore pressure model to analyse the pore pressures, these models can be used for the future drilling wells in pre-drill pore pressure predictions.
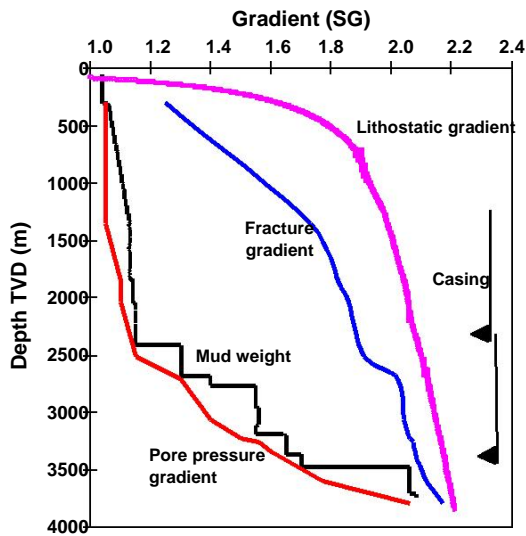
Figure 2. Pore pressure gradient, fracture gradient, overburden stress gradient (lithostatic gradient), mud weight, and casing shoes with depth (Zhang 2011: 52)

2.3 REVIEW OF SOME METHODS OF PORE PRESSURE PREDICTION

The first pore pressure prediction approach was derived by Hottmann and Johnson (1965), they were derived this approach for shale formations based on well log data such as velocity, resistivity and acoustic travel time. Their approach derived and initiated in Upper Texas and Southern Louisiana Gulf Coast of Miocene and Oligocene shale formations, they specified one specification was related to porosity and depth. If depth increases, the porosity decreases means decreasing of porosity is function of depth. The relationship between porosity and depth was called normal compaction trend, this tendency signifies normal compaction trend was function of depth and fluid pressure in burial depths showed in normal trend is called hydrostatic pressure. The normal compaction trend's subsequent data points are deviate, when the abnormal compaction intervals are penetrated. If fluid pressure in formation is abnormally high, the intervals of abnormal compaction are resisted the porosity of shale at abnormally high depths.

Hottmann and Johnson (1965), Gardner et al. (1974) were proposed an equation to predict the formation pore pressure based on analysing the data. That can be written as in the following form:

$$p_f = \sigma_v - [(\sigma_v - \beta)(A_1 - B_1 \ln \Delta t)^3 \div Z^2] \qquad (2)$$

Where, the formation fluid pressure (p_f) expressed in psi; the overburden stress (σ_V) expressed in psi; the normal overburden stress gradient (α_V) expressed in psi/ft; the normal fluid pressure gradient (β) expressed in psi/ft; the depth (Z) expressed in ft; the sonic transit time (t) expressed in μs/ft; A, B are the constants, A_1 =82,776 and B_1 =15,695.

Afterward, many pore pressure prediction methods, models and empirical equations were obtained based on well logging data such as: resistivity, interval velocity, sonic transit time and other data. In the below sections explained and discussed the some normally used pore pressure prediction methods based on properties of shale.

2.3.1 Pore pressure prediction from resistivity

The Gulf of Mexico, North Sea basins are called young sedimentary basins, in these basins overpressure is foremost problem due to under-compaction. In young sedimentary basins pore pressure prediction can predict properly by using well-log-based resistivity method. Eaton (1972, 1975) proposed an equation for shale formations to predict pore pressure gradient using resistivity log data, this equation can be written in the following form:

$$P_{pg} = OBG - (OBG - P_{ng}) \, (R \div R_n)^n \qquad (3)$$

Where, the formation pore pressure gradient (P_{pg}) expressed in psi/ft; the overburden stress gradient (OBG) expressed in psi/ft; the hydrostatic pore pressure gradient (P_{ng}), (normally 0.45 psi/ft or 1.03 MPa/km, dependent on water salinity); the shale resistivity (R) found from well log; the shale resistivity at the normal (hydrostatic) pressure (R_n); the exponent (n) varied from 0.6 to 1.5, and normally n =1.2.

Predominantly in young sedimentary basins, Eaton's resistivity method is valid to predict the pore pressure pore certainly the normal shale resistivity is appropriately estimated (e.g., Lang et al. 2011). These are two approaches to predict the pore pressure, the first approach is the normal shale resistivity is assume as constant, the second approach is the normal compaction trend line determine accurately.

2.3.2 Pore pressure prediction from interval velocity and transit time

Eaton's method
Eaton (1975) proposed an equation to predict pore pressure gradient from sonic transit time. That empirical equation can be written in the following form:

$$P_{pg} = (OBG - P_{ng}) \, (\Delta t_n \div \Delta t)^3 \qquad (4)$$

Where, the sonic transit time (t_n) at the normal pressure; the sonic transit time (t) gotten from well log in shale, and the sonic transit time (t) can obtain by using seismic interval velocity. Transit time based pore pressure gradient prediction method limited in geologically complex areas such as uplift formations. It does appropriate in certain petroleum fields and this method does not study unloading effects. The normal transit time is needed to apply this method.

Bowers' method
In Gulf of Mexico basin, Bowers (1995) determined and analysed the effective stresses, sonic interval velocities by using measured pore pressure data, well logging data of shale and overburden stress. Bowers presented an equation related to effective stress and sonic velocity, that relationship can be written in the following form:

$$V_p = V_{ml} + A\sigma_e^{\ B} \qquad (5)$$

Where, the compressional velocity at a given depth (v_p); the compressional velocity in the mudline (v_{ml}) (the mudline means sea floor or the ground surface, normally $v_{ml} \approx 5000$ ft/s, or 1520 m/s); A and B are the parameters standardised with offset velocity versus effective stress data.

Substituting σ_e value in equation (5) ($\sigma_e = \sigma_V - p$), then rearrange equation (5) to obtain the pore pressure from the velocity as termed in Eq. (5), as:

$$P = \sigma_v - ((v_p - v_{ml}) \div A)^{1/B} \qquad (6)$$

The constant values A =10–20 and B =0.7–0.75 for Gulf of Mexico basin. Substitute $10^6/t$ for v_p and $10^6/t_{ml}$ for v_{ml} to convert the equation (6) in form of transit time.

$$P = \sigma_V - [(10^6(\frac{1}{\Delta t} - \frac{1}{\Delta t_{ml}}) \div A)]^{1/B} \qquad (7)$$

Where, the compressional transit time in the mudline (t_{ml}), t_{ml} values are generally 200 μs/ft or 660 μs/m.

At the same effective stress, the loading curve seems greater than the velocity and where unloading or formation uplift occurs, the compressional velocity and effective stress can not follow the loading curve. An empirical equation proposed to explanation for the effect of unloading curves by Bowers (1995):

$$V_P = V_{ml} + A\,[\sigma_{max}(\sigma_e/\sigma_{max})^{1/U}]^B \qquad (8)$$

Where, the uplift parameter (U); and

$$\sigma_{max} = ((v_{max} - \bar{v}_{ml}) \div A)^{1/B}$$

Where, the effective stress (σ_{max}) and velocity (v_{max}) are the estimates at the onset unloading. v_{max} is generally fixed identical to the velocity, where major lithology changes are absent.

The pore pressure can be achieved by rearranging equation (8) in the unloading case:

$$P_{ulo} = \sigma_v - (\frac{v_p - v_{ml}}{A})^{U/B} (\sigma_{max})^{1-U} \qquad (9)$$

Where, the pore pressure for the unloading case (p_{ulo}).

In shallow formation velocity is very slow and pore pressure overestimated because this formation is poor and consolidated. The Gulf of Mexico and many other basins applied Bowers method.

Miller's method

Miller sonic or seismic method defines a relationship for formation pore pressure and sonic or seismic transit time, this relationship developed between velocity and effective stress. Maximum velocity depth (d_{max}) is a control parameter to unloading and it is an input

parameter in Miller's sonic method. The condition to not occurring unloading, maximum velocity depth should be less than the depth (Z). Miller sonic method equation to predict the pore pressure can be written as in the following form (Zhang et al. 2008):

$$P = \sigma_v - \frac{1}{\lambda} \ln \left(\frac{v_m - v_{ml}}{v_m - v_p} \right) \qquad (10)$$

Where, the sonic interval velocity (v_m), normally v_m value: 14,000– 16,000 ft/s; the compressional velocity at a given depth (v_p); the empirical parameter (λ), normally $\lambda = 0$; the depth at which the unloading has occurred (d_{max}).

Unloading behaviour is assumed at maximum velocity is greater than depth. In the unloading case, the pore pressure can be determined from the bellow equation:

$$P_{ulo} = \sigma_v - \frac{1}{\lambda} \ln \left[a_m \left(1 - \frac{v_p - v_{ulo}}{v_m - v_{ml}} \right) \right] \qquad (11)$$

Where, the ratio of loading and unloading slopes of velocities in the effective stress curves (a_m), generally $a_m = 1.8$; the effective stress from unloading of the sediment (σ_{ul}); the velocity where unloading begins (v_{ulo}).

Tau model:

Shell proposed a pore prediction method based on velocity. Shell introduced a "Tau" variable, this variable used in the effective stress equation (Lopez et al, 2004; Gutierrez et al, 2006):

$$\Sigma_e = A_S \tau^B{}_s \qquad (12)$$

Where, the fitting constants are (A_s, B_s); the Tau variable is (τ), and $\tau = (C-\Delta t) / (\Delta t-D)$; the compressional transit time obtained from sonic log or seismic velocity is (Δt); the mudline transit time (C), generally C = 200 µs/ft, it is constant; and the matrix transit time (D), generally D = 50 µs/ft, it is constant.

Then the pore pressure can be calculated from equation, that is:

$$P = \sigma_v - A_s \left(\frac{C-\Delta t}{\Delta t-D} \right)^B{}_s \qquad (13)$$

The best fitting parameters in the Gulf of Mexico are A_s = 1989.6 and B_s = 0.904 (Gutierrez et al. 2006).

The benefit in Tau model and Millers model is the consideration of mudline and matrix effects in pore pressure prediction and   Tau model, Millers model both are comparable to Bower's method.

2.3.3 Adapted Eaton's methods with depth-dependent normal compaction trendlines

Eaton's resistivity method with depth-dependent normal compaction trendline:

Eaton's primary equation in hydrostatic pore pressure case, is challenging to define the resistivity or normal resistivity of shale. A new approach to determine the normal resistivity of shale is assumed as constant of normal shale resistivity. Though, the normal resistivity of shale is a constraint of formation depth and it is in many cases not constant. Therefore for the pore pressure prediction the normal compaction trendline should be require to determine.

Measured resistivity is a function of burial depth, based on this a relationship developed between burial depth and measured resistivity for normal pressured formations. The resistivity's normal compaction trend line equation can be following in the form:

$$\text{Ln } R_n = \ln R_o + bZ \quad \text{or } R_n = R_0 e^{bZ} \tag{14}$$

Where, In the case of normal compaction, the shale resistivity is (R_n); the resistivity of shale in the sea floor is (R_0); the constant is (b); and the depth below the sea floor is (Z).

The Eaton's resistivity equation can be stated by substituting equation (14) into $p_{FPmax} = 2\sigma_{min} - p$ in the following equation:

$$P_{pg} = OBG - (OBG - P_{ng}) \left(\frac{R}{R_0 e^{bZ}}\right)^n \tag{15}$$

Where, at depth Z, the measured shale resistivity is (R); in the sea floor the normal compaction shale resistivity is (R_0); the slope of logarithmic resistivity normal compaction trendline is (b).

Eaton's velocity method with depth-dependent normal compaction trendline:

In the subsurface formations the velocity rises with burial depth. The phenomenon predicted by Slotnick (1936) was that represents the compressional velocity is depends on depth. Thus, the travel time's normal compaction trendline must be a constraint of depth. Slotnick (1936) proposed a linear relationship of seismic velocity's first and easy normal compaction trendline in the below equation:

$$V = V_0 + kZ \tag{16}$$

Where, at depth Z, the seismic velocity is (v); the velocity at the sea floor is (v_0); constant is (k).

The normal pressured velocity relationship proposed by Sayers et al. (2002) to predict the pore pressure. In Carnarvon Basin established a relationship for depth dependent shale acoustic travel time. This exponential relationship established from 17 normally pressured

wells (van Ruth et al. 2004):

$$\Delta t_n = 225 + 391e^{-0.00103Z} \tag{17}$$

Where, the acoustic transit time is (t_n) expressed in µs/m; depth is (Z) expressed in meters.

The normal pore pressure formations of sonic transit time measured data used to propose the general relationship of transit time's normal compaction as following:

$$\Delta t_n = \Delta t_m + (\Delta t_{ml} - \Delta t_m)e^{-cZ} \tag{18}$$

Where, the compressional transit time is (t_m) in the formation matrix shale (porosity is zero); the sea floor transit time is (t_{ml}); and here the constant is (c).
The Eaton's modified sonic correlation can be stated in the below form:

$$P_{pg} = OBG - (OBG - P_{ng})\left(\frac{\Delta t_m + (\Delta t_{ml} - \Delta t_m)e^{-cZ}}{\Delta t}\right)^3 \tag{19}$$

2.3.4 New theoretical models of pore pressure prediction

Pore pressure prediction from porosity:

The basic reasons to occur overpressure in formation are mainly in basins dropping quickly and low permeability of rocks, the under compaction is one more cause to overpressured formations. Higher pore pressure and greater porosity of formation are the main indicators to identify the under-compaction, those are greater in under-compaction than in the normal compaction condition. In normal compacted formations if exponentially depth increases the formation porosity decreases, this statement generally accepted (e.g., Athy. 1930):

$$\phi = \phi_0 e^{-cZ} \tag{20}$$

Where, porosity is φ; the porosity in the sea floor is φ_0; the true vertical depth below the sea floor is Z; the compaction constant is c, usually it is 1/m or 1/ft.

The similar connection be existent in porosity and effective stress (e.g., Dutta. 2002; Flemings et al. 2002; Peng and Zhang. 2007).

$$\Phi = \phi_0 e^{-a\sigma_e} \tag{21}$$

Here, the stress compaction constant is (a) and this value is 1/psi or 1/MPa.

As introduced before, the pore pressure and effective stress are indication of porosity, principally hydrocarbon cracking and under-compaction are caused to create overpressures. Thus, formation porosity played key role in estimation of pore pressure. The identification of

under-compaction, formation overpressure are demonstrated from porosity profile in Figure 3. The overpressure generation and occurrence of under-compaction happened by the reason of porosity reversed. The cause for top of overpressure or under compaction is reversal of porosity point initial stage. There is a difference in normal compaction and under compaction, in the normal compaction formations pore pressure and porosity are lower than the under compaction formations.
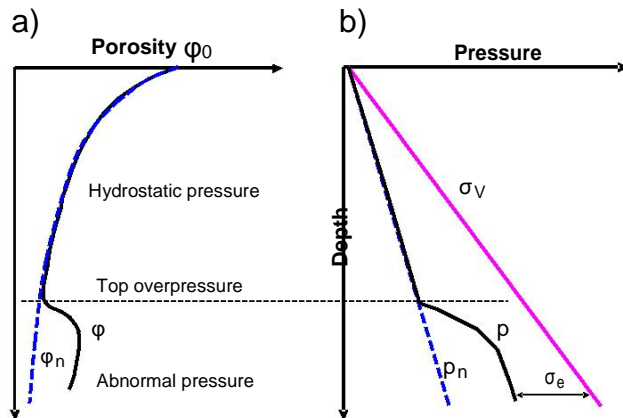
Figure 3. Schematic porosity (a) and corresponding pore pressure (b) in a sedimentary basin. (Zhang 2011:59)

Pore pressure prediction by using porosity data in mudstone and shale formations needed some efforts. Here some examples mentioned, pore pressure prediction based on porosity dependent effective stress model proposed by Holbrook et al. (2005). Pore pressure prediction model based on shale porosity data developed in the form of empirical porosity equation which are equal to Eaton's sonic model, that model proposed by Heppard et al. (1998). Porosity stress relationship developed for mudstone formations to predict the overpressures is proposed by Flemings et al. (2002) and Schneider et al. (2009).

Zhang. (2008) proposed porosity based pore pressure prediction theoretical model allowing to porosity normal compaction trend line. The author's theoretical equation can be calculate to the pressure gradient, that equation can be written as in the following form:

$$P_{pg} = OBG - (OBG - P_{ng}) \frac{ln\phi_0 - ln\phi}{cZ} \qquad (22)$$

Here, the porosity in shale is φ at depth Z, this be able to attain from sonic or density logs, the porosity in the sea floor is ϕ_0; the depth below the sea floor is Z; the normal compaction porosity trendline gives c value.

The below equation can be written in terms of porosity, overburden stress and pore pressure:

$$P = \sigma_v - (\sigma_v - p_n) \frac{ln\phi_0 - ln\phi}{cZ} \qquad (23)$$

The above equation can be calculated pore pressure that is depth dependent equation to calculate the pore pressure. This is the basic difference to above equation and other porosity-pore pressure equations. In addition to that, porosity normal compaction trend line is indicator of depth.

The indication of formation overpressured, if the porosity (φ) is greater at chosen depth compared with the normal porosity (φ_n) at the same chosen depth, this is called the formation is overpressured. The below equation used to generate the normal compaction porosity trendline for overpressured formations:

$$\Phi_n = \phi_0 e^{-cZ} \qquad (24)$$

Pore pressure prediction from transit time or velocity:

Density logs, sonic logs and seismic interval velocity data are required to collect Porosity data. Raiga-Clemenceau et al. (1988) proposed an equation to generate porosity by using transit time or compressional velocity. Porosity can be calculated from the following equation:

$$\phi = 1 - \left(\frac{\Delta t_m}{\Delta t}\right)^{1/x} \qquad (25)$$

Here, the exponent (x) can be obtained from the data. Issler (1992) proposed exponent x value as 2.19 at fixed transit time value t_m =67 μs/ft for Mackenzie Delta of northern Canada.

From velocity or compressional transit time, the pore pressure calculated by rearranging equation (25) and (22):

$$p_{pg} = OBG - (OBG - P_{ng}) \frac{C_m - \ln[1 - \left(\frac{\Delta t_m}{\Delta t}\right)^{\frac{1}{x}}]}{cZ} \qquad (26)$$

Here, the compressional transit time in the matrix, the transit time in the sea floor is (C_m). Where, it can be written as $C_m = \ln[1 - (t_m / t_{ml})^{1/x}]$.

Wyllie et al. (1956) proposed an empirical equation for porosity estimation.

$$\phi = \frac{\Delta t - \Delta t_m}{\Delta t - \Delta t_m} \qquad (27)$$

Here, the transit time of fluid is Δt_f

The pore pressure gradient and pore pressure are calculated from Wyllie's porosity-transit time equations. These equations can be written in following correlations:

$$p_{pg} = OBG - (OBG - P_{ng}) \frac{\ln(\Delta t_{ml} - \Delta t_m) - \ln(\Delta t - \Delta t_m)}{cZ} \qquad (28)$$

$$p = \sigma_v - (\sigma_v - p_n) \frac{\ln(\Delta t_{ml} - \Delta t_m) - \ln(\Delta t - \Delta t_m)}{cZ} \qquad (29)$$

The below equation can be used to calculate the normal compaction trendline of the transit time:

$$\Delta t_n = \Delta t_m + (\Delta t_{ml} - \Delta t_m)e^{-cZ} \qquad (30)$$

The advantages of this model is at higher depths normal transit time reaches the matrix transit time because of normal compaction trend, this method physically approved Chapman (1983). The main difference to other methods and this method, in this method normal compaction trendline is used and compaction mechanism better for sediments. The additional benefits of this method is depth dependent to calculate pore pressures and consideration of matrix, mudline transit time effects.

2.3.5 Formation Fracture Gradient Prediction Strategy

Formation fracture pressure mandatory to crack the formation and the disadvantage of fracture pressure is mud losses, this is caused by high fracture pressure. If fracture pressure is high the mud entered from wellbore to made Fracture. Normally, fracture pressures are calculated by using models, however fracture gradients can be calculated by fracture pressure divided with the true vertical depth (TVD). The fracture gradient means maximum mud weight and the main advantage of fracture gradient generally used in three fields, which are drilling planning, while drilling and mud weight design. The wrong formation fracture gradient estimation leads to tensile failure, mud losses or lost circulation, these can be happened in the case of mud weight value is greater than the formation fracture gradient. Formation fracture pressure measured by using many tests and approaches, such as downhole leak-off test (LOT) and the minimum stress method, tensile failure method. In drilling industry basically used two methods, that are (1) the minimum stress method. (2) The tensile failure method.

Minimum stress for lower bound of fracture gradient:

The tensile strength of rock property does not discuss in the minimum stress method, it only discuss about the pressure to fracture the formation and extend the already fractured the formation. Hence, the lower bound of fracture pressure signifies the minimum stress. The

fracture closure pressure is naturally equal to the minimum stress, this principal detected in leak-off test resulting the breakdown pressure (Zhang et al. 2008). Hubbert and Willis (1957), Eaton (1968) and Daines (1982) proposed methods are comparable to the minimum stress method.

$$\sigma_{min} = \frac{v}{1-v}(\sigma_v - p) + p \qquad (31)$$

Here, the lower bound of fracture pressure is σ_{min}; the Poisson's ratio is v.
The fracture gradient is lesser than minimum stress, in the case of open fracture occur in the formation. The effective stress coefficient variable presented in fracture gradient prediction equation by Matthews and Kelly (1967).

$$p_{FG} = k_0\big(OBG - P_{pg}\big) + P_{pg} \qquad (32)$$

Here, the formation fracture gradient is P_{FG}; the formation pore pressure gradient is P_{pg}; the overburden stress gradient is OBG; the effective stress coefficient is K_0, $K_0 = \sigma_{min}'/\sigma_V'$; the minimum effective in-situ stress is σ_{min}'; the effective overburden stress is σ_V.
The effective stress coefficient values resultant based on fracture threshold values, and obtained in the field from leak-off test.

Formation breakdown pressure for upper bound of fracture gradient:

The mud loss occurred in the wellbore first when the fractured occured in undamaged formations. Kirsch's solution applied in the case of minimum tangential stress is equal to the tensile strength and to calculate the fracture pressure and fracture gradient (Haimson and Fairhurst. 1970; Zhang and Roegiers. 2010). In leak-off test the fracture pressure is called fracture breakdown pressure (Zhang et al. 2008). In vertical well drilling the upper bound fracture pressure can be calculated from following equation:

$$p_{FPmax} = 3\sigma_{min} - \sigma_H - p - \sigma_T + T_0 \qquad (33)$$

Here, the upper bound of fracture pressure is P_{FPmax}; the maximum horizontal stress is σ_H; the minimum horizontal stress is σ_{min}; the thermal stress is σ_T; brought by the difference between the mud temperature and the formation temperature, and the tensile strength of the rock is T_0.
Assumed, the maximum horizontal stress is equal to the minimum horizontal stress and ignore tensile strength and temperature effect. Now, the equation (33) can be written in the following equation:

$$p_{FPmax} = 2\sigma_{min} - p \qquad (34)$$

The upper bound of fracture pressure can be written by rearranging the equations (31) and (34) to express as:

$$p_{FPmax} = \frac{2v}{1-v}(\sigma_v - p) + p \qquad (35)$$

The single variation between the fracture pressure of upper bound and fracture pressure of lower bound is a constant value before effective vertical stress. The fracture gradient of upper bound is called the bound of lost circulation or the maximum fracture gradient (Zhang et al. 2008).

Hence, the fracture pressure of lower bound and the fracture pressure of upper bound average is probably considered fracture pressure. This fracture pressure equation can be expressed as follows:

$$P_{FP} = \frac{3v}{2(1-v)}(\sigma_v - p) + p \qquad (36)$$

Here, the probably fracture pressure is P_{FP}.

The suggested models have been applied in some petroleum basins such as Gulf of Mexico, North Sea, for validation of models. The pore pressures in the shale formations, deep fields and hydraulically not connected shales are overpressure. In the shale formations compaction disequilibrium occurred due to overpressures, thus the fluid flow theory cannot be predict the pore pressures. However, in shale formations to predict the pore pressures generally used shale petrophysical data and well logs. Normal compaction trend lines can be easily handled by using Eaton's resistivity and sonic methods. In the case of the compaction disequilibrium has been reason to overpressure generation, the pore pressure prediction depends on theoretical pore pressure-porosity model as the fundamental theory in shale formations. Pore pressure prediction model based on porosity and compressional velocity (sonic transit time) models are using this theoretical pore pressure-porosity model. Well logging data and suitable method selection provided accurate results with required calibrations in several case studies.

CHAPTER 3

3. 0 METHODOLOGY

Based on literature review done, it is basically clear that there are two models of assessing pore pressure prediction on Judy and Jade fields in the Central Graben Area of the North Sea.

These models are:
- Pore pressure prediction from porosity
- Tau model

3.1 PORE PRESSURE PREDICTION FROM POROSITY

Porosity based pore pressure prediction model is one of the new theoretical model. Conventional porosity-based pore pressure analysis using sonic or seismic velocity and resistivity data as a measure of porosity retention, under- estimates the overpressure effect of these secondary overpressure mechanisms. This methodology to identify overpressure generation mechanisms in the Judy and Jade fields by using depth versus porosity plotting, and discuss implications for pre-drill prediction, also review approaches to allow for these mechanisms. This model mechanism examine on available data of Judy and Jade fields to determine pore pressures. The calculated pore pressure data compare with the available pore pressure data of these both fields, to assess the validation of model in Judy, Jade fields.

3.2 TAU MODEL

Tau model is a velocity dependent pore pressure prediction method, this model was proposed by Shell. The advantage of Tau model is the effects of both the matrix and mudline velocities are considered on pore pressure prediction. This model examined by calculating the pore pressures by using overburden stress data of Judy and Jade fields and plot the graph depth versus pore pressure gradient. Compare this generated plot with available data of these fields.

The purpose of this project work, emphasis will be placed in exploring pore pressure prediction models, in order to predict and analyse as an approach to high pressure, high temperature wells. These two pore pressure prediction models are new and advanced approaches of pore pressure prediction from well logs. The verified and recommended model objective is to improve the drilling performance for these fields.

The approach for this work is going to be based on the chart below, these steps are key for verifying the data and to deliver the best result.

```
                    ┌─────────────────────────────┐
                    │   Pore pressure prediction   │
                    └──────────────┬──────────────┘
              ┌────────────────────┴────────────────────┐
┌──────────────────────────┐              ┌──────────────────────────┐
│  Pore pressure prediction │              │        Tau model         │
│  from porosity model      │              │                          │
└─────────────┬─────────────┘              └─────────────┬────────────┘
┌──────────────────────────┐              ┌──────────────────────────┐
│  Plot a graph porosity    │              │  Calculate pore pressure │
│  (vs.) depth              │              │  from the equation       │
└─────────────┬─────────────┘              └─────────────┬────────────┘
┌──────────────────────────┐              ┌──────────────────────────┐
│  Calculate pore pressure  │              │  Calculate the pore      │
│  gradient from the equation│             │  pressure gradient       │
└─────────────┬─────────────┘              └─────────────┬────────────┘
┌──────────────────────────┐              ┌──────────────────────────┐
│  Plot a graph depth (vs)  │              │  Plot a graph depth (vs) │
│  pore pressure gradient   │              │  pore pressure gradient  │
└─────────────┬─────────────┘              └─────────────┬────────────┘
              └──────────────┐    ┌──────────────────────┘
                    ┌────────────────────────────┐
                    │  Compare the pore pressure  │
                    │  gradients with available data│
                    └──────────────┬──────────────┘
                    ┌────────────────────────────┐
                    │   Select the suitable model  │
                    └──────────────┬──────────────┘
                    ┌────────────────────────────┐
                    │  Calculate the fracture     │
                    │  gradients by using equation │
                    └──────────────┬──────────────┘
                    ┌────────────────────────────┐
                    │  Plot the graph depth       │
                    │  (vs) gradients             │
                    └──────────────┬──────────────┘
                    ┌────────────────────────────┐
                    │  Conclusion and             │
                    │  Recommendations            │
                    └────────────────────────────┘
```

CHAPTER 4

4. 0 DISCUSSION AND ANALYSIS

The study zone is situated in quadrant 30 (Great Britain), 300 km east-southeast of Aberdeen (Figure 4), and contains in its deeper sections a high-pressure high-temperature region (HPHT). This region is portion of a greater field with HPHT environments, focussed in the profounder Mesozoic segments of the Central Graben and in the southern portion of the Viking Graben.

The extremely overpressured Mesozoic (pre-rift) clastic reservoirs at 4-5 km burial depths are of Triassic and Middle Jurassic age (Triassic Heron Group and Middle Jurassic Brent Group), and range temperatures up to 194°C. These are highly overpressured reservoirs. Petroleum accretions enclose wet gas condensates and black oils. The Upper Jurassic syn-rift shales of the Humber Group, the major source rocks in the Central Graben area (Kimmeridge Clay; Heather formation, Pentland coals), overlie the pre-rift strata. The Upper Cretaceous Chalk Group, consisting primarily of chalks and marls, overlays the pre- and syn-rift strata, and is provincially an operative pressure seal in the Central Graben area (Darby, et al. 1996; Mallon and Swarbrick.2002; Swarbrick, et al. 2000).
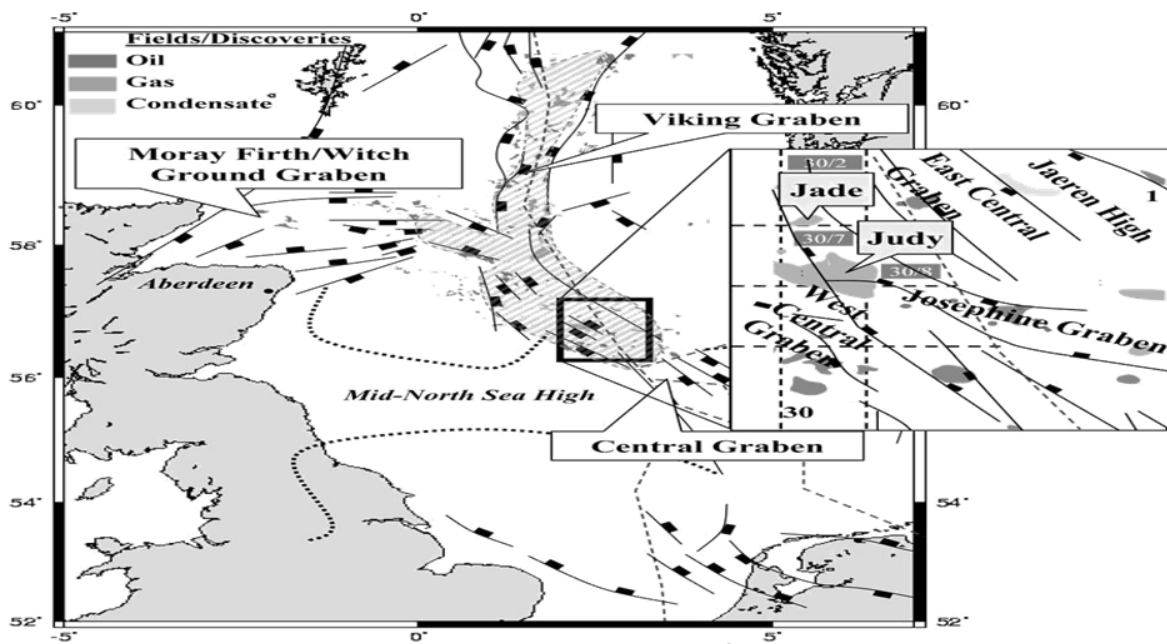

Figure 4. Study area of Judy and Jade fields (International journal of earth sciences 2008).

The geology of Jade and Judy fields have been discussed extensively in the literature (Jones et al. 2005; Swarbrick et al. 2000). Briefly, the Jade structure consists of three NW-SE dipping, tilted fault blocks. The main reservoir is the Joanne sandstone, belonging to the upper part of the Triassic Skagerrak Formation. Reservoir pore pressures exceed 800 bars and temperatures are above 166°C at the reservoir apex, and reach values of up to 200°C in the deeper sections, as measured in production tests. The Judy field is located on a horst block approximately 20 km south of Jade. Multiple Triassic Skagerrak Formation reservoir units occur, consisting mainly of medium grained quartz-rich sandstones interrupted by shaly sequences. Locally also Jurassic Fulmar sandstone reservoirs are developed. The field is segmented by faults into individual compartments which contain highly variable fluid types, ranging from black oils to gas condensates. Pore pressures in the pre-Cretaceous reservoirs exceed 600 bar and temperatures are around 150°C.

4.1 THE JUDY FIELD

The Judy field located in Block 30/7a in Quadrant 30 of the UK North Sea, 175 miles east-southeast of Aberdeen. In 1985 hydrocarbons were discovered by the 30/7a-4a well on the Judy Field. Excellent flow rates were obtained from both the Pre-Cretaceous Jurassic and Triassic sands. These sands along with the Joanne formations were subsequently appraised by seven more wells drilled between 1985 and 1992, revealing the Judy Pre-Cretaceous reservoir as a complex fault compartmentalized structure.
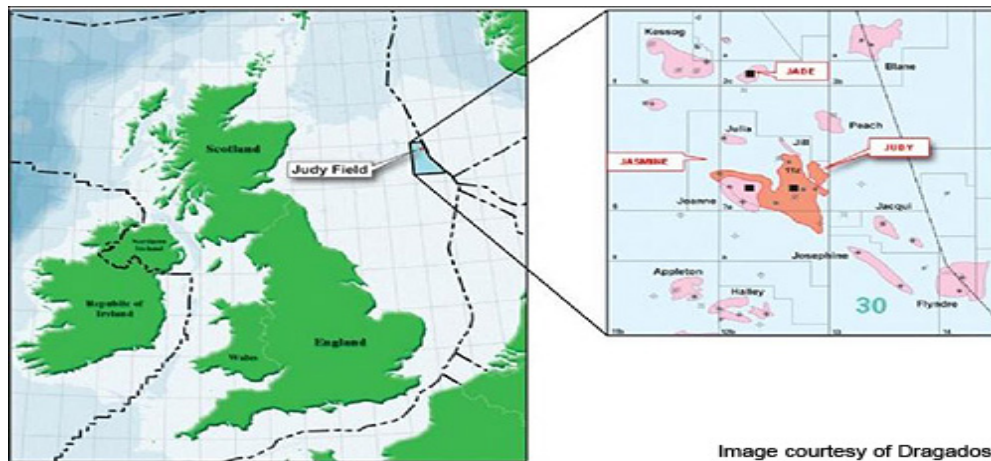

Figure 5. Judy field area (Offshore technology.com 2012).

4.2 THE JADE FIELD

The Jade Field is an example of a high pressure high temperature heterogeneous fluvial reservoir which, at the time of development, appeared to be a straight-forward case of production by natural depletion. The Jade Field is a high pressure/high temperature (HPHT) gas/condensate field located in the East Central Graben of the North Sea in UKCS Licence Block 30/2c, 270km east of Aberdeen (Figure 6). The field is operated by ConocoPhillips (32.5%) and the remaining ownership consists of BG (35%), Chevron (19.93%), Eni (7%) and OMV (5.57%). The field was discovered in 1996 by well 30/2c-3 and appraised in 1997 by well 30/2c-4. First production was achieved in 2002 through a normally unmanned production wellhead platform connected to the Judy processing facilities in Block 30/7a by a 17km pipeline (Jones et al. 2005).

Figure 6. Location of Jade field and its surrounding fields (Charles 2010).

4.3 PORE PRESSURE PREDICTION BASED ON POROSITY MODEL:

4.3.1 Judy field:
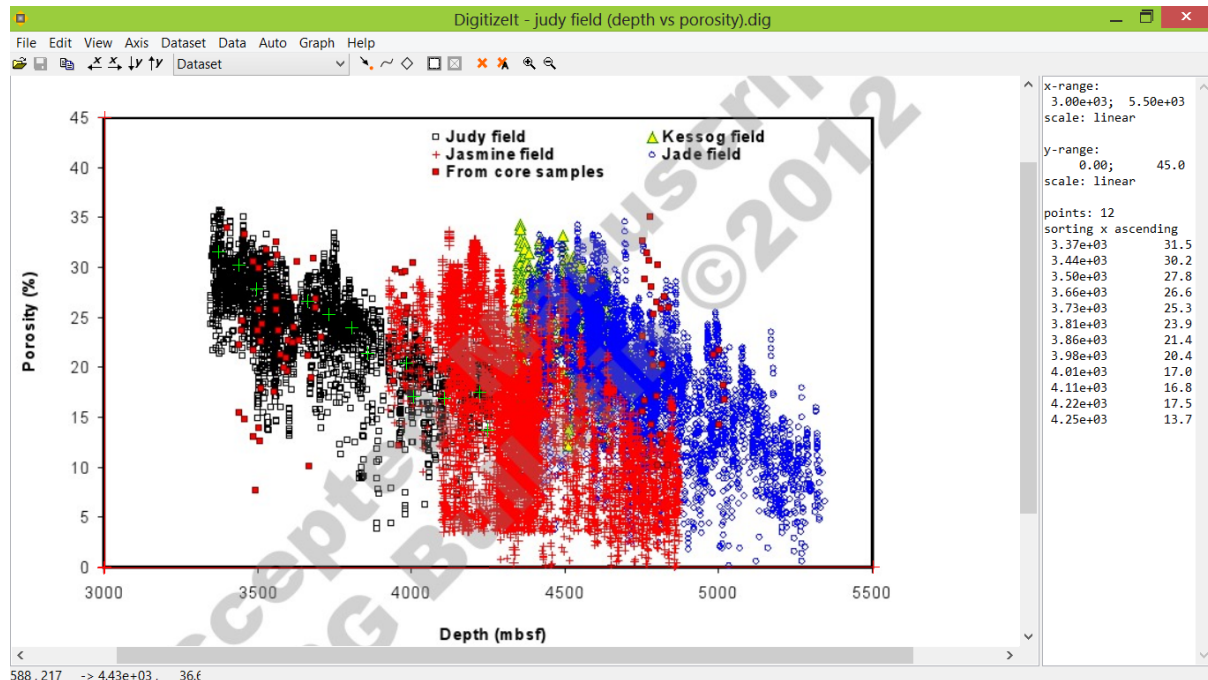
Figure 7. Judy field porosity percentage (Nguyen 2013).

This figure gives the data of porosity (%) along with depth (mbsf). For better understanding and convenience of calculations, change the units of porosity (fractions) and depth (ft mbsf).

DEPTH (mbsf)	POROSITY (%)	DEPTH (ftbsf)	POROSITY (fraction)
3370	31.5	11056.4	0.135
3440	30.2	11286.0	0.302
3500	27.8	11482.9	0.278
3660	26.6	12007.8	0.266
3730	25.3	12237.5	0.253
3810	23.9	12500.0	0.239
3860	21.4	12664.0	0.214
3980	20.4	13057.7	0.204
4010	17.0	13156.1	0.170
4110	16.8	13484.2	0.168
4220	17.5	13845.1	0.175
4250	13.7	13943.5	0.137

Table 1. Judy field depth-porosity data.

This table prepared from figure (7), this data extracted from available figure by using Digitalizeit software.

Porosity of shale:
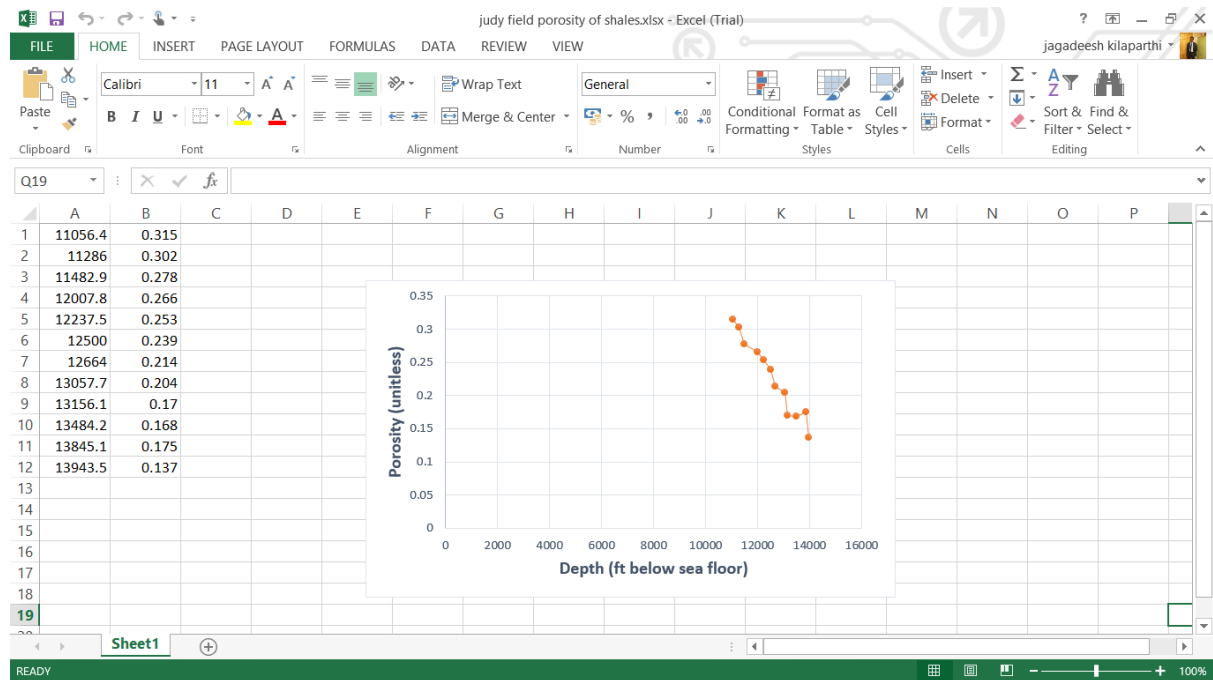
Figure 8. Judy field depth versus porosity graph

Depth (ftbsf)	Porosity
11056.4	0.135
11286.0	0.302
11482.9	0.278
12007.8	0.266
12237.5	0.253
12500.0	0.239
12664.0	0.214
13057.7	0.204
13156.1	0.170
13484.2	0.168
13845.1	0.175
13943.5	0.137

Table 2. Judy field porosity data.   Plot 1. Judy field depth versus porosity.
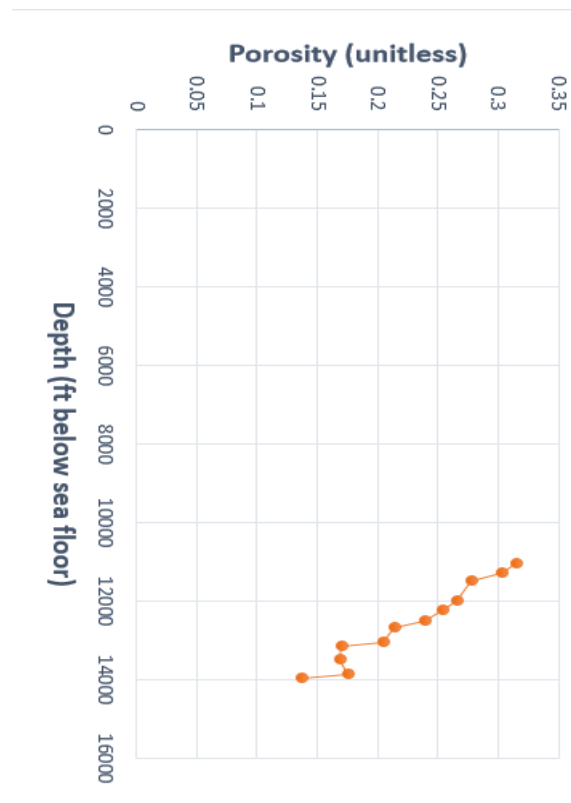
Judy field depth versus porosity plot (1) showing, the porosity is decreasing with respect to increasing of depth from the available data.

Normal compaction trendline of porosity:

The normal compaction porosity trendline can be determined from the following equation:

$$\Phi_n = \phi_0 e^{-cZ}$$ where, φ_0=0.55 and c=0.00024 (Yardley, Swarbrick 2000)

Depth(ftbsf)	Normal porosity
0	0.55
1000	0.43
2000	0.34
3000	0.26
4000	0.21
5000	0.16
6000	0.13
7000	0.10
8000	0.08
9000	0.06
10000	0.04
11000	0.03
12000	0.03
13000	0.02
14000	0.01

Table 3. Judy field normal porosity.
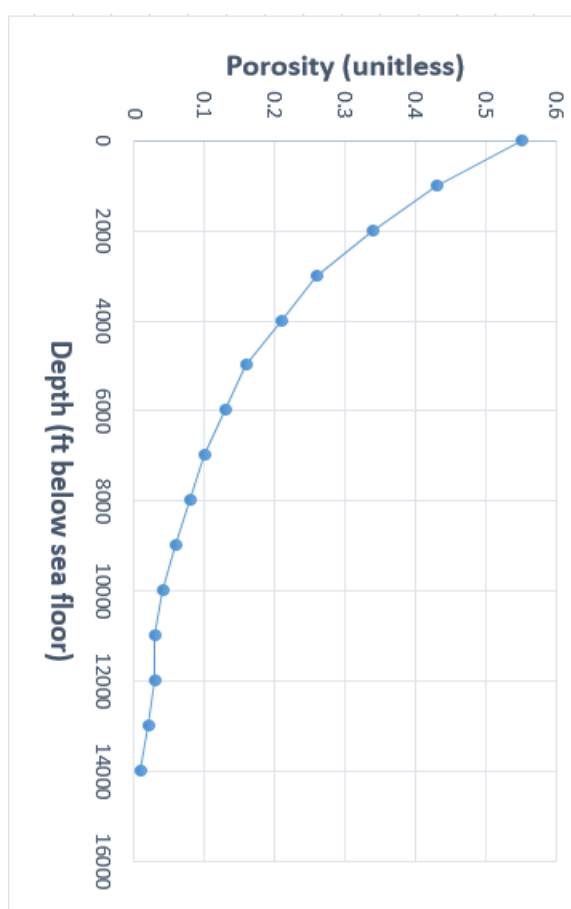
Plot 2. Judy field normal trend line.

The normal compaction trend line (plot 2) of Judy field is showing, the porosity is decreases along with depth from surface porosity. This means, if depth is increases the porosity is decreasing and at high depths the porosity percentage is completely decrease.

Pore pressure gradients:

The pore pressure gradient can be calculated from the following equation:

$$P_{pg} = OBG - (OBG - P_{ng})\frac{ln\phi_0 - ln\phi}{cZ}$$ where, P_{ng}= 0.434psi/ft, OBG= 1psi/ft (Daniel 2000)
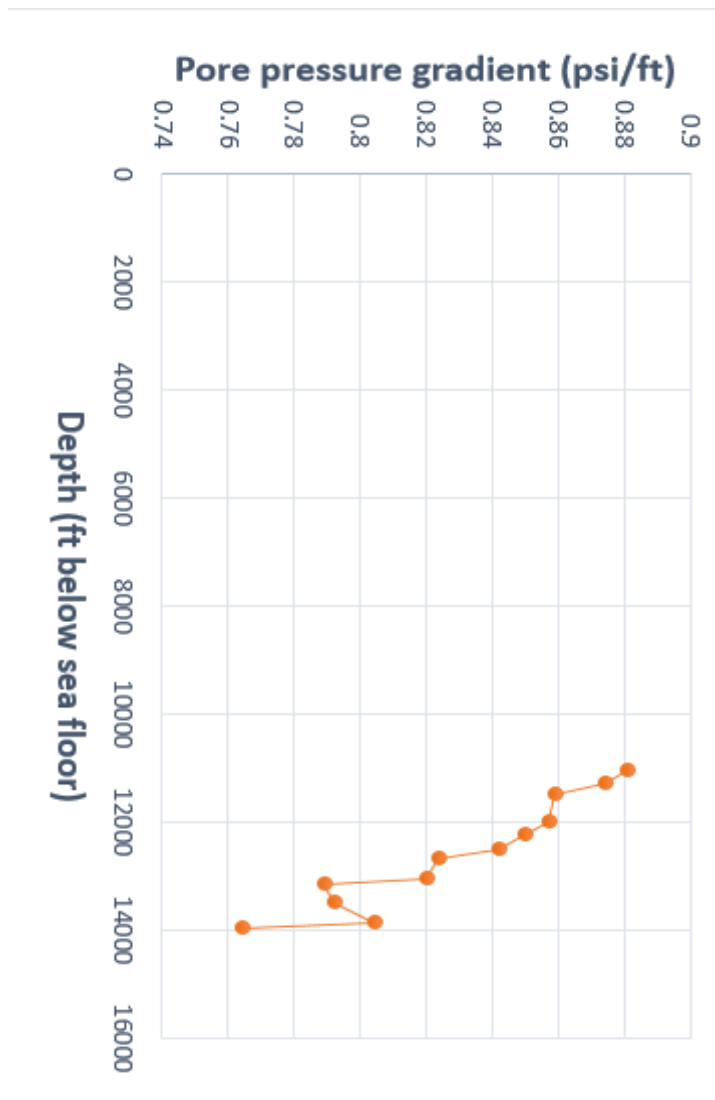
Depth (ftbsf)	Pore pressure gradient (psi/ft)
11056.4	0.881
11286.0	0.874
11482.9	0.859
12007.8	0.857
12237.5	0.850
12500.0	0.842
12664.0	0.824
13057.7	0.820
13156.1	0.789
13484.2	0.792
13845.1	0.804
13943.5	0.764

Table 4. Judy field pore pressure gradient.

Plot 3. Judy field pore pressure gradient trend line.

Pore pressure prediction from porosity model gave the result for Judy field, the pore pressure gradient values (plot 3) are decreasing with respect to depth. However, the fundamental theory (figure 2) explained, the pore pressure gradient trend line increases with depth. Thus, the porosity based pore pressure prediction model gave incorrect result for Judy field.

4.3.2 JADE FIELD:

Porosity based pore pressure prediction model verification on Jade field.
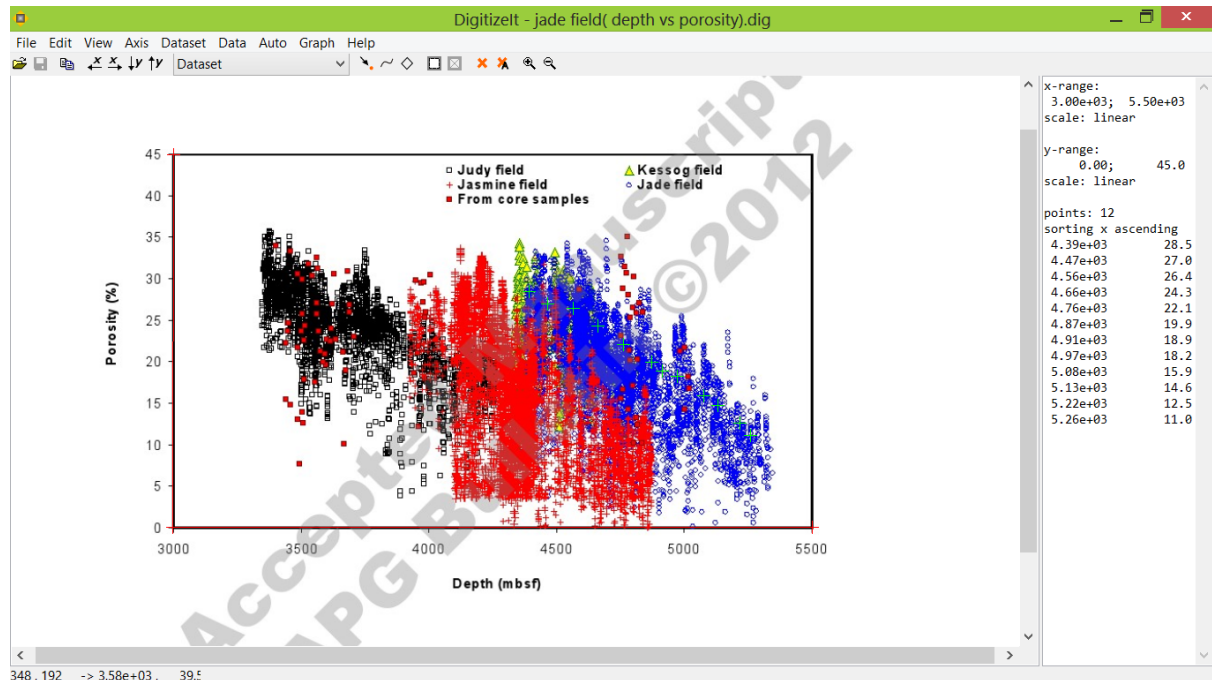
Figure 9. Jade field porosity percentage (Nguyen 2013).

Extracted data of depth (mbsf) and porosity (%) convert in terms of depth (ftbsf) and porosity (fraction).

Depth (mbsf)	Porosity (%)	Depth (ftbsf)	Porosity (fraction)
4390	28.5	14402.8	0.285
4470	27.0	14665.3	0.270
4560	26.4	14960.6	0.264
4660	24.3	15288.7	0.243
4760	22.1	15616.7	0.221
4870	19.9	15977.6	0.199
4910	18.9	16108.9	0.189
4970	18.2	16305.7	0.182
5080	15.9	16666.6	0.159
5130	14.6	16830.7	0.146
5220	12.5	17125.9	0.125
5260	11.0	17257.2	0.110

Table 5. Jade field depth-porosity data.

Porosity of shale:
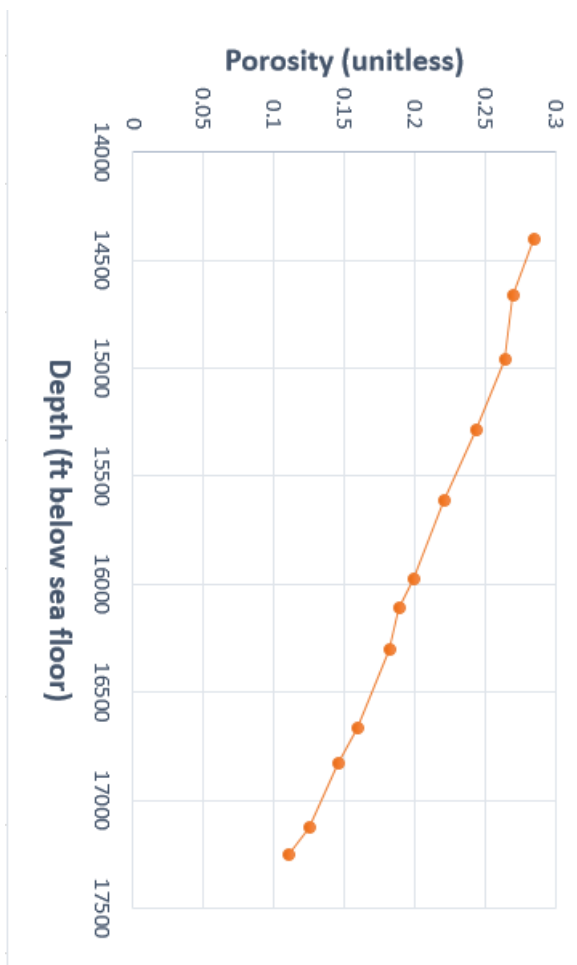
Depth (ftbsf)	Porosity
14402.8	0.285
14665.3	0.270
14960.6	0.264
15288.7	0.243
15616.7	0.221
15977.6	0.199
16108.9	0.189
16305.7	0.182
16666.6	0.159
16830.7	0.146
17125.9	0.125
17257.2	0.110

Table 6. Jade field porosity data.

Plot 4. Jade field porosity trend line.

Jude field depth versus porosity plot (4) shows, the porosity is decreasing with respect to increasing of depth from the available data. Which are extracted data (figure 9) by using Digitalizeit software.

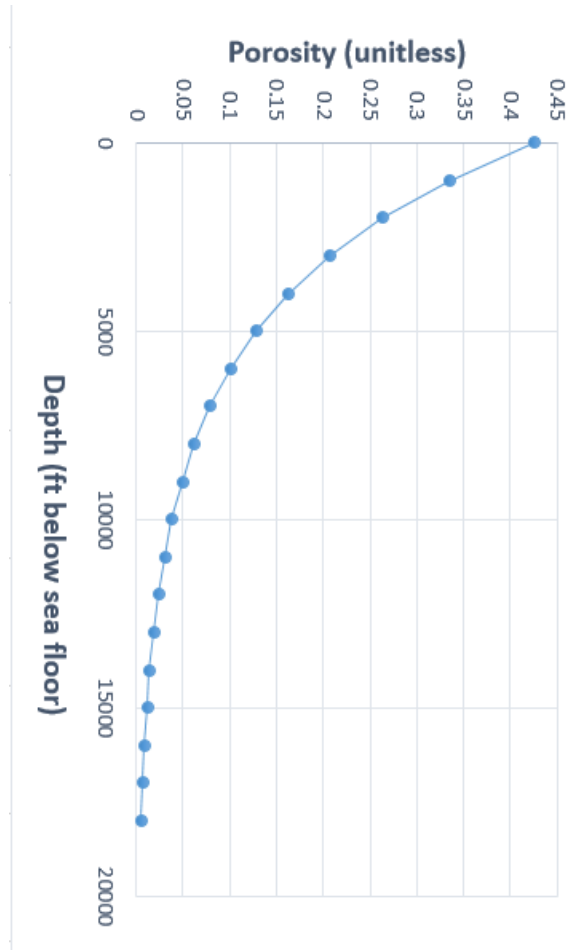**Normal compaction trendline of porosity**:

The normal compaction porosity trendline can be determined from the following equation:

$$\Phi_n = \phi_0 e^{-cZ} \text{ where, } \varphi_0 = 0.425 \text{ and } c = 0.00024 \text{ (Yardley, Swarbrick 2000)}$$

Depth (ftbsf)	Normal porosity
0	0.425
1000	0.334
2000	0.262
3000	0.206
4000	0.162
5000	0.128
6000	0.100
7000	0.079
8000	0.062
9000	0.049
10000	0.038
11000	0.030
12000	0.023
13000	0.018
14000	0.014
15000	0.011
16000	0.009
17000	0.007
18000	0.005

Plot 5. Jade field normal porosity trend line.

Table 7. Jade field normal porosity.

The normal compaction trend line (plot 5) of Jude field is showing, the porosity is decreases along with depth from surface porosity. This means, if depth is increases the porosity is decreasing and at high depths the porosity percentage is completely decreased.

Pore pressure gradients:

The pore pressure gradient can be calculated from the following equation:

$$P_{pg} = OBG - (OBG - P_{ng})\frac{\ln\phi_0 - \ln\phi}{cZ}$$

Where, P_{ng} = 0.434psi/ft, OBG = 1psi/ft (Daniel 2000)

Depth (ftbsf)	Pore pressure gradient (psi/ft)
14402.8	0.934
14665.3	0.927
14960.6	0.924
15288.7	0.913
15616.7	0.901
15977.6	0.888
16108.9	0.881
16305.7	0.857
16666.6	0.848
17125.9	0.831
17257.2	0.815
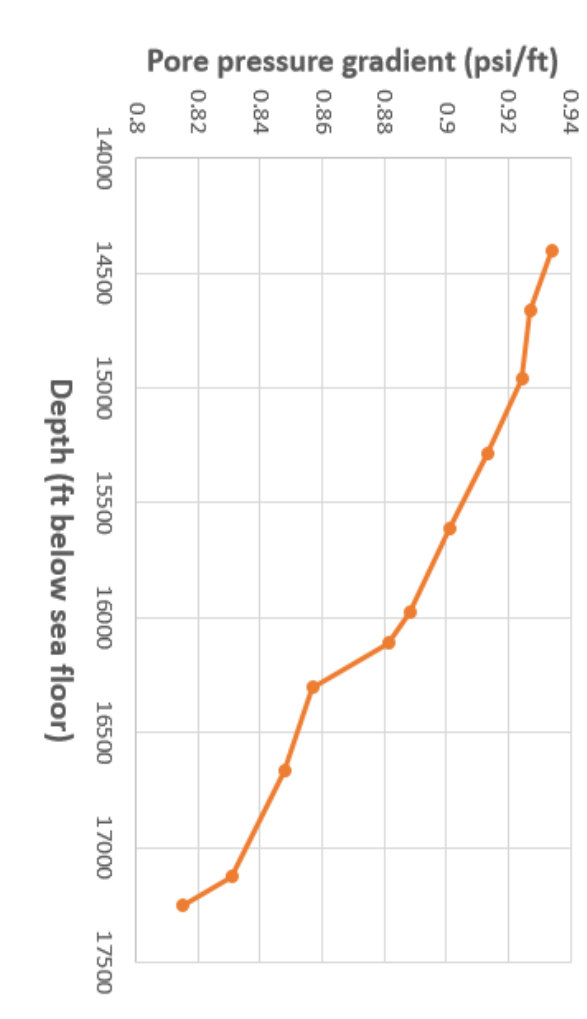
Table 8. Jade field pore pressure gradient. Plot 6. Jade field pore pressure gradient trend line

Pore pressure prediction from porosity model gave the result for Judy field, the pore pressure gradient values (plot 6) are decreasing with respect to depth. However, the fundamental theory (figure 2) explained, the pore pressure gradient trend line increases with depth. Thus, the porosity based pore pressure prediction model gave incorrect result for Jude field.

4.4 ANALYSIS OF TAU MODEL:

4.4.1 Estimation of overburden stress of Judy and Jade fields from diagram:
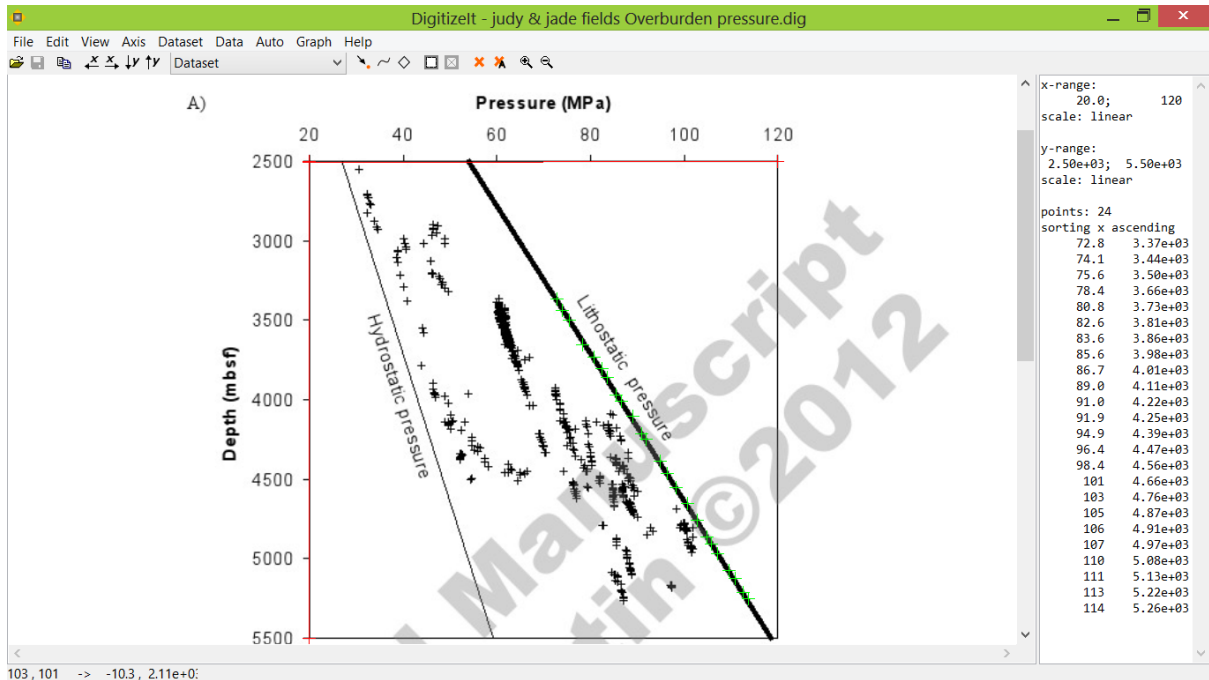
Figure 10. Judy and Jade field's lithostatic pressure data (Nguyen 2013).

Overburden stress of Judy field:

Depth (ftbsf)	Overburden stress (psi)
11056.4	10558.74
11286.0	10747.29
11482.9	10964.85
12007.8	11370.95
12237.5	11719.04
12500.0	11980.11
12664.0	12125.15
13057.7	12415.22
13156.1	12574.76
13484.2	12908.35
13845.1	13198.43
13943.5	13328.96

Table 9. Judy field overburden pressure data.

Judy field overburden (lithostatic) pressure data generated by using the Digitalizeit software from figure 10. This data (table 10) shows, the overburden pressure is increased along with depth.

Overburden stress of Jade field:

Depth (ftbsf)	Overburden stress (psi)
14402.8	13764.07
14665.3	13981.63
14960.6	14271.70
15288.7	14648.80
15616.7	14938.88
15977.6	15228.95
16108.9	15373.99
16305.7	15519.03
16666.6	15954.14
17125.9	16389.26
17257.2	16534.29

Table 10. Jade field overburden pressure data.

Jude field overburden (lithostatic) pressure data generated by using the Digitalizeit software from figure 10. This data (table 11) shows, the overburden pressure is increased along with depth.

4.4.2 Estimation of Pore Pressure and Pore Pressure Gradients of Judy and Jade fields:

Pore pressure can be calculated from using this equation:

$$P = \sigma_v - A_s\left(\frac{C-\Delta t}{\Delta t - D}\right)^{B_s}$$

Judy field pore pressure and pore pressure gradients:

Depth (ftbsf)	Pore pressure (psi)	Pore pressure gradient (psi/ft)
11056.4	8109.77	0.733
11286.0	8298.32	0.735
11482.9	8515.88	0.741
12007.8	8921.98	0.743
12237.5	9270.07	0.757
12500.0	9531.14	0.762
12664.0	9676.18	0.764
13057.7	9966.25	0.763
13156.1	10125.79	0.769
13484.2	10459.38	0.775
13845.1	10749.46	0.776
13943.5	10879.99	0.780
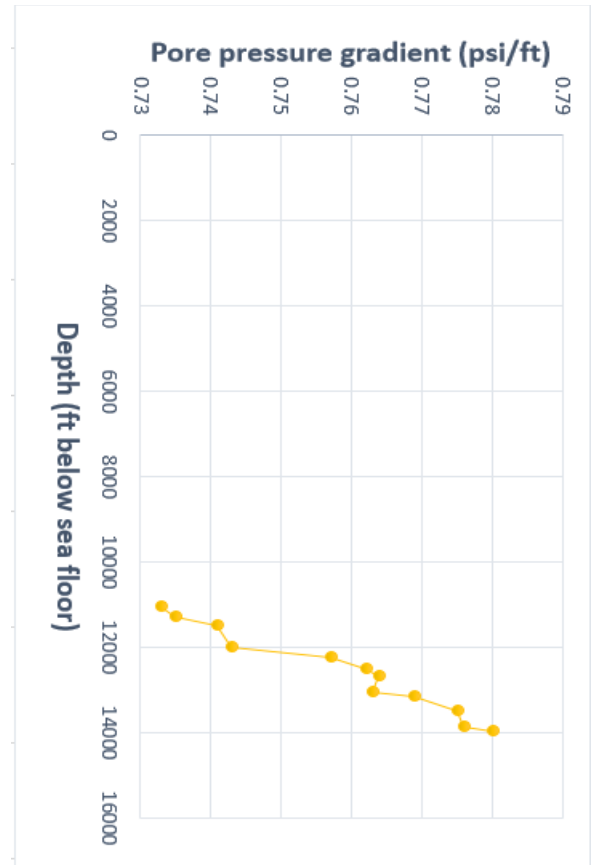
Plot 7. Judy field pore pressure gradient trend line.

Table 11. Judy field pore pressure gradients.

Tau Model applied on Judy field, this model gave reliable results for Judy field pore pressure gradient trend line (plot 7). This pore pressure gradient trend line increased with depth for Judy field. However, the fundamental theory (figure 2) explained, the pore pressure gradient trend line increased with depth. Thus, the Tau model gave correct result for Judy field.

Jade field pore pressure and pore pressure gradients:

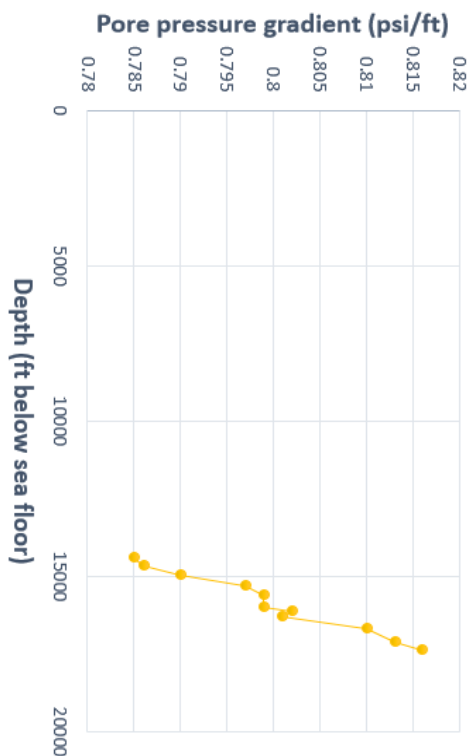| Depth (ftbsf)	Pore pressure (psi)	Pore pressure gradients (psi/ft)
14402.8	11315.10	0.785
14665.3	11532.66	0.786
14960.6	11822.73	0.790
15288.7	12199.83	0.797
15616.7	12489.91	0.799
15977.6	12779.98	0.799
16108.9	12925.02	0.802
16305.7	13070.06	0.801
16666.6	13505.17	0.810
17125.9	13940.29	0.813
17257.2	14085.32	0.816

Table 12. Jade field pore pressure gradient.

Plot 8. Jade field pore pressure gradient trend line.

Tau Model applied on Jude field, this model gave reliable results for Jude field pore pressure

gradient trend line (plot 8). This pore pressure gradient trend line increased with depth for Jade field. However, the fundamental theory (figure 2) explained, the pore pressure gradient trend line increased with depth. Thus, the Tau model gave correct result for Jade field.

4.5 ANALYSIS OF AVAILABLE DATA

Pore pressure gradients from available data of Judy and Jade fields:
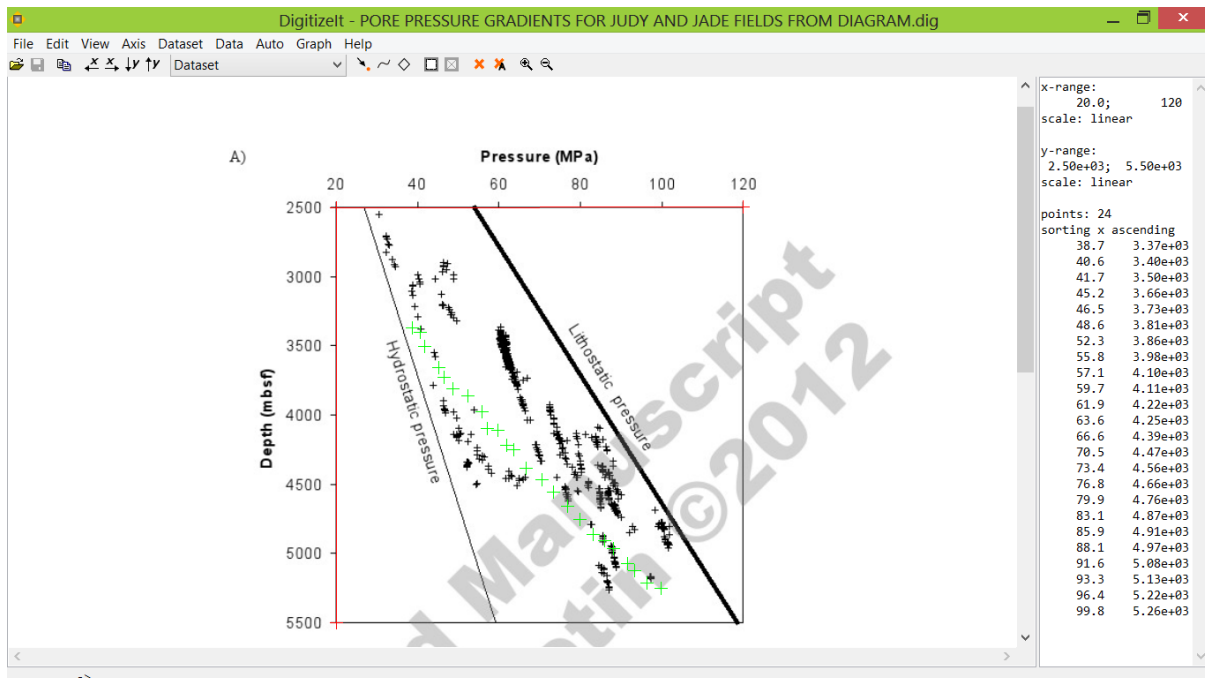
Figure 11. Judy and Jade fields pore pressure data (Nguyen 2013).

4.5.1 Pore pressure gradients for Judy field:

From above diagram depths and pressures converted to feet and psi successively.

Depth (ft below sea floor)	Pore pressure (psi)	Pore pressure gradient (psi/ft)
11056	5612.958	0.507
11286.0	5888.530	0.521
11482.9	6048.072	0.526
12007.8	6555.704	0.545
12237.5	6744.253	0.551
12500.0	7048.832	0.563
12664.0	7585.471	0.598
13057.7	8093.103	0.619
13156.1	8281.652	0.629
13484.2	8658.750	0.642
13845.1	8977.833	0.648
13943.5	9224.397	0.661

Table 13. Judy field pore pressure gradient.
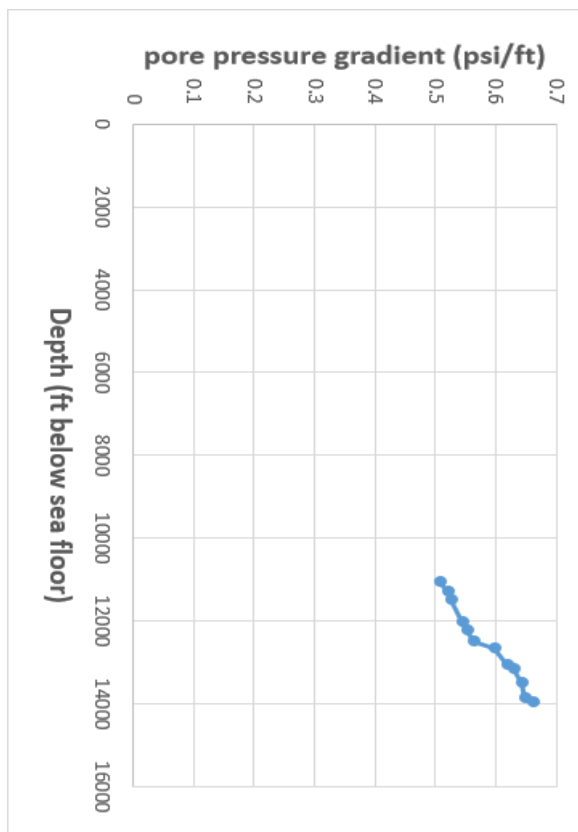
Plot 9. Judy field pore pressure gradient trend line.

Judy field's pore pressure gradient trendline (plot 9) showed, the pore pressure gradient values increased with respect to depth. This pore pressure gradient data for Judy field generated from figure 10, by using Digitalizeit software.

4.5.2 Pore pressure gradients for Jade field:

Depth (ft below sea floor)	Pore pressure (psi)	Pore pressure gradient (psi/ft)
14402.8	9659.510	0.670
14665.3	10225.157	0.697
14960.6	10645.767	0.711
15288.7	11138.895	0.728
15616.7	11588.512	0.742
15977.6	12052.632	0.754
16108.9	12458.738	0.773
16305.7	12777.821	0.783
16666.6	13285.453	0.797
16830.7	13532.017	0.804
17125.9	13981.634	0.816
17257.2	14474.762	0.838

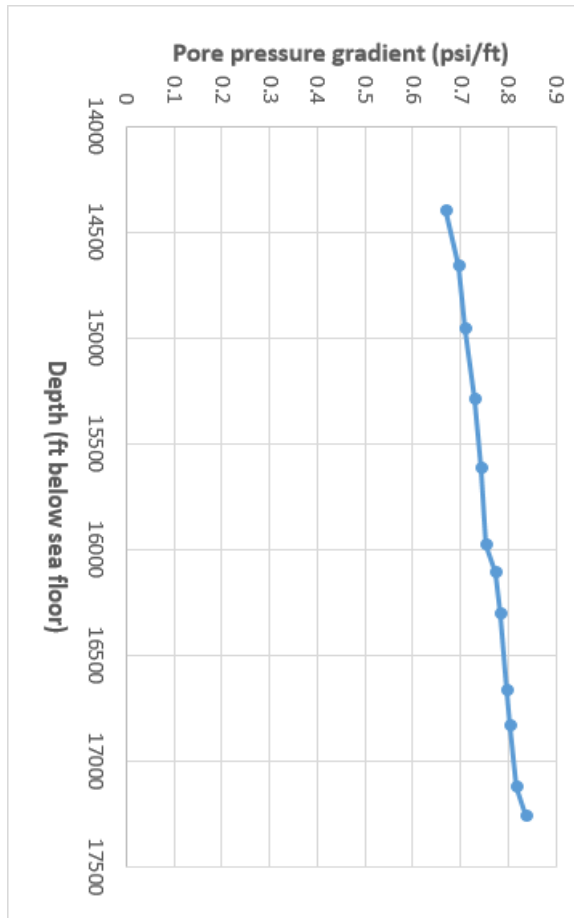Table 14. Jade field pore pressure gradient.

Plot 10. Jade field pore pressure gradient trend line.

Jade field's pore pressure gradient trendline (plot 10) showed, the pore pressure gradient values increased with respect to depth. This pore pressure gradient data for Jade field generated from figure 10, by using Digitalizeit software.

4.6 COMPARISON OF PORE PRESSURE GRADIENT RESULTS

4.6.1 Comparison of pore pressure gradient plots for Judy field:

Comparison of available data pore pressure gradient plot and porosity based pore pressure prediction model plot:
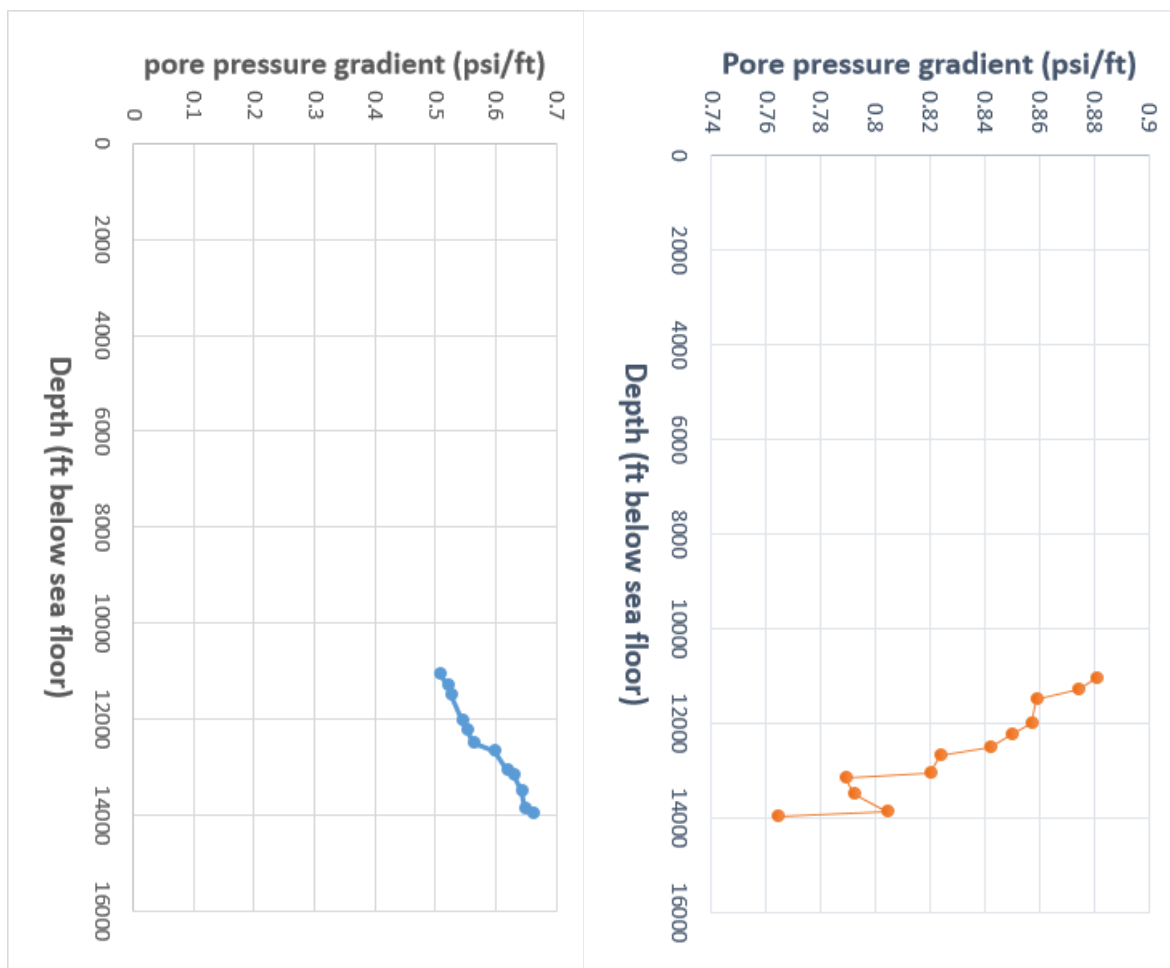
Plot 11. Judy field pore pressure gradients comparison of available data and porosity based pore pressure prediction model.

The comparison of pore pressure gradient trend lines (plot 11) generated from available data and pore pressure prediction from porosity model showed, the quite opposite trend lines. This means, the pore pressure prediction from porosity model gave incorrect result for Judy field.

Comparison of available data pore pressure gradient plot and Tau model pore pressure gradient plot:

Plot 12. Judy field pore pressure gradients comparison of available data and Tau model.

The comparison of pore pressure gradient trend lines (plot 12) generated from available data and Tau model showed, the quite parallel trend lines. This means, the Tau model gave correct result for Judy field.

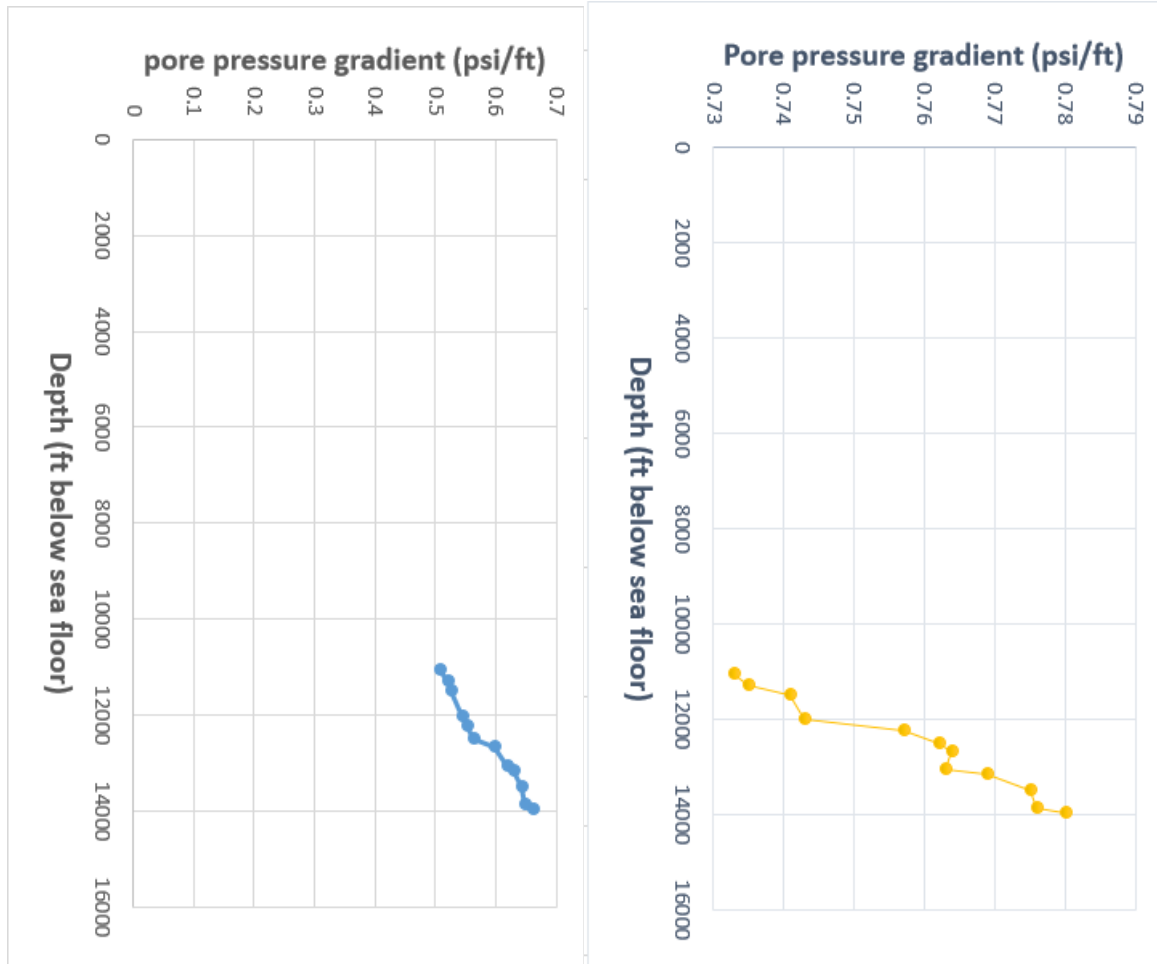## 4.6.2 Comparison of pore pressure gradient plots for Jade field:

Comparison of available data pore pressure gradient plot and porosity based pore pressure prediction model plot:

Plot 13. Jade field pore pressure gradients comparison of available data and porosity based pore pressure prediction model.

The comparison of pore pressure gradient trend lines (plot 13) generated from available data and pore pressure prediction from porosity model showed, the quite opposite trend lines. This means, the pore pressure prediction from porosity model gave incorrect result for Jade field.

Comparison of available data pore pressure gradient plot and Tau model pore pressure gradient plot:
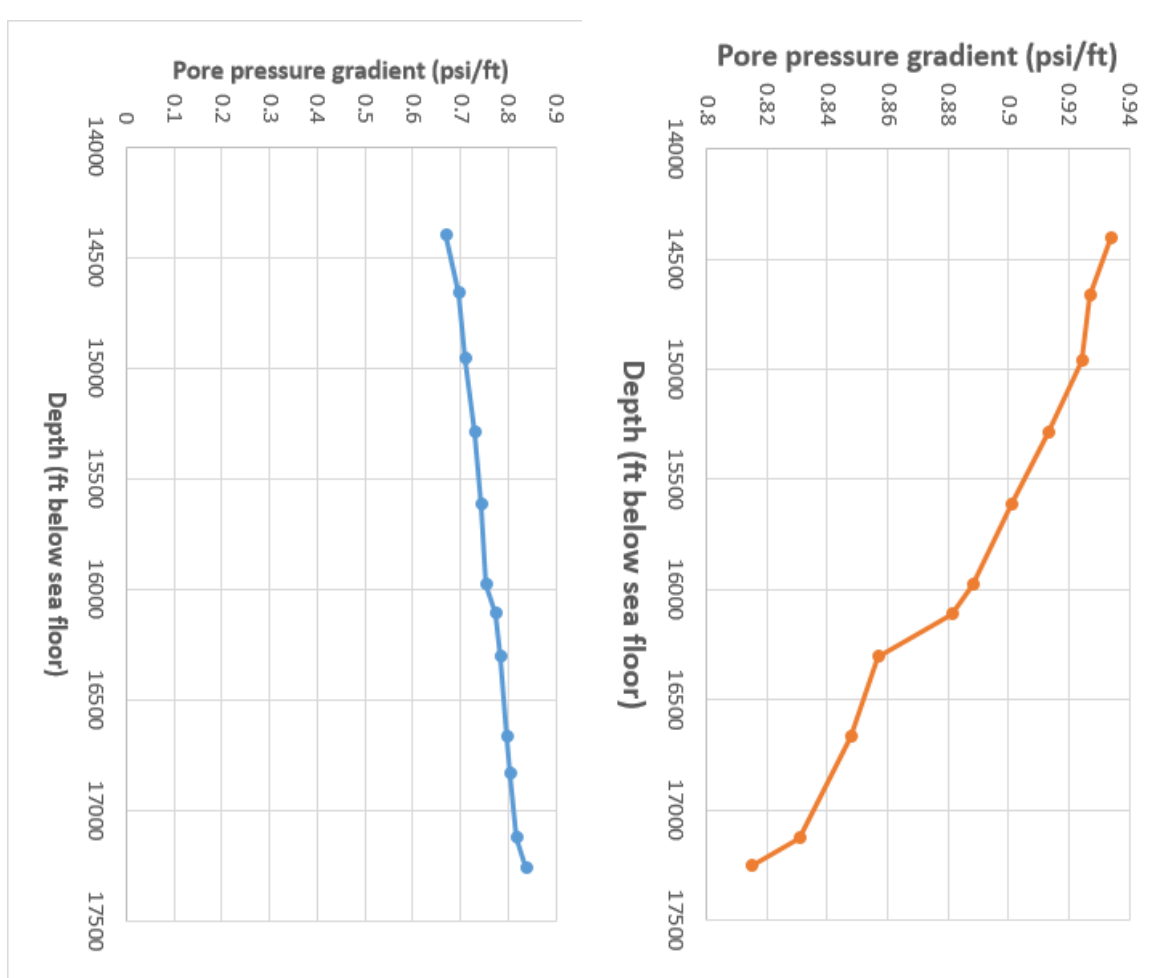

Plot 14. Jade field pore pressure gradients comparison of available data and Tau model.

The comparison of pore pressure gradient trend lines (plot 14) generated from available data and Tau model showed, the quite parallel trend lines. This means, the Tau model gave correct result for Jade field.
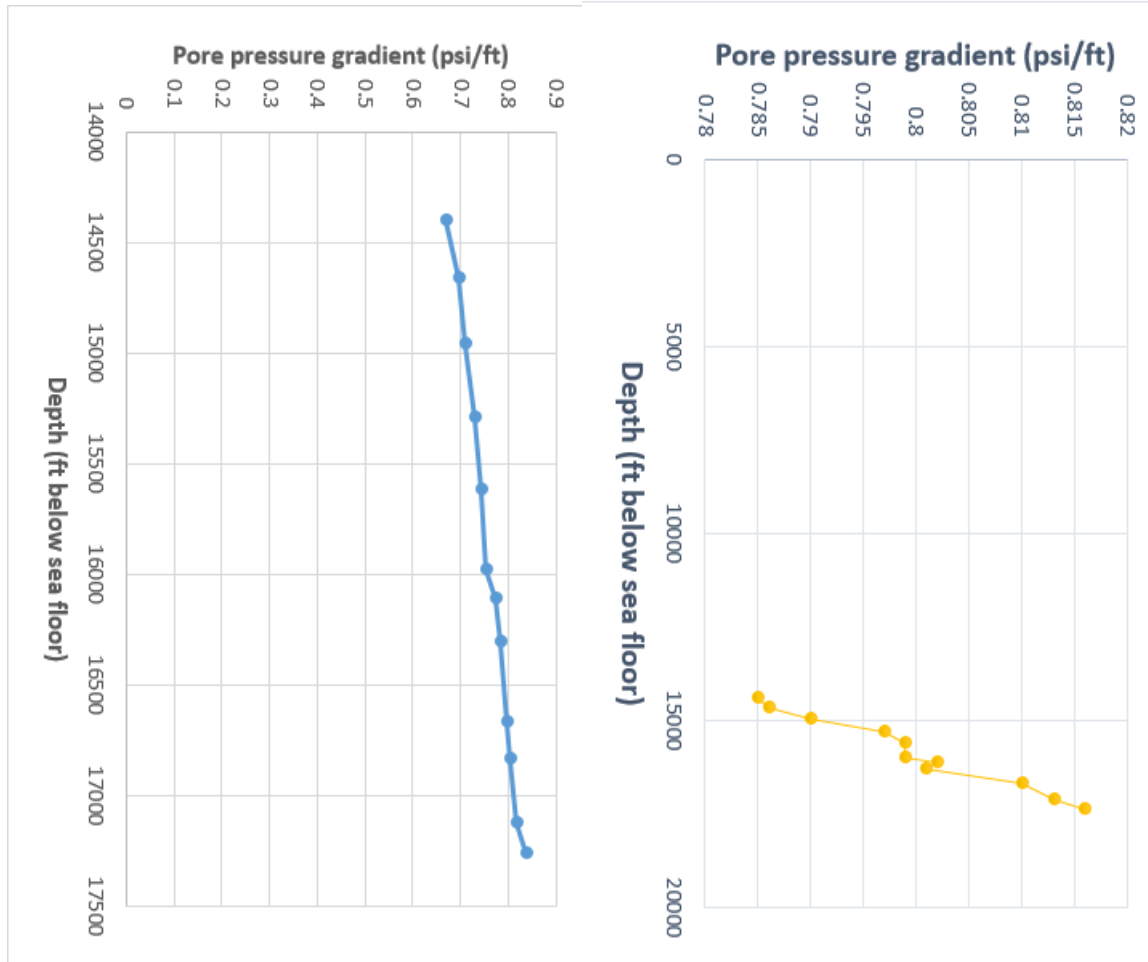
4.7 COMPARISON OF PORE PRESSURE GRADIENTS INTERMS OF PERCENTAGE

The pore pressure gradients comparison between available data and Tau model, because Tau model pore pressure gradient trendlines similar to available data pore pressure gradient trendlines. Thus, the similarity of these pore pressure gradient trendlines calculated in terms of percentage for both Judy and Jade fields.

4.7.1 Judy field pore pressure gradients comparison in terms of percentage:

Depth (Ftbsf)	Available data pore pressure gradients (psi/ft)	Tau model pore pressure gradients (psi/ft)	Difference of pore pressure gradients (%)
11056.4	0.507	0.733	44.57
11286.0	0.521	0.735	41.07
11482.9	0.526	0.741	40.87
12007.8	0.545	0.743	36.33
12237.5	0.551	0.757	37.38
12500	0.563	0.762	35.34
12664	0.598	0.764	27.75
13057.7	0.619	0.763	23.26
13156.1	0.629	0.769	22.25
13484.2	0.642	0.775	20.71
13845.1	0.648	0.776	19.75
13943.5	0.661	0.780	18.00

Table 15. Judy field pore pressure gradients comparison of available data and Tau model.

The above table indicating the difference between available data pore pressure gradients and Tau model pore pressure gradients. From this table one remarkable point observed, that point is if the depth increases but the difference of pore gradients in terms of percentage decreased.

4.7.2 Jade field pore pressure gradients comparison in terms of percentage:

Depth (Ftbsf)	Available data pore pressure gradients (psi/ft)	Tau model pore pressure gradients (psi/ft)	Difference of pore pressure gradients (%)
14402.8	0.670	0.785	17.16
14665.3	0.697	0.786	12.76
14960.6	0.711	0.790	11.1
15288.7	0.728	0.797	9.47
15616.7	0.742	0.799	7.68
15977.6	0.754	0.799	5.96
16108.9	0.773	0.802	3.75
16305.7	0.783	0.801	2.29
16666.6	0.797	0.810	1.63
17125.9	0.816	0.813	-0.003
17257.2	0.838	0.816	-0.002

Table 16. Jade field pore pressure gradients comparison of available data and Tau model.

The key observation from this table, the pore pressure gradients difference in terms of percentage completely decreased to reach the zero percentage.

4.8 Estimation of Fracture gradients for Judy and Jade fields

Finally, chosen Tau model to both Judy and Jade fields, because always pore pressure gradients increase along with depth. By the observation, porosity based pore pressure prediction model failed to satisfy this condition in both Judy and Jade fields. Tau model verified and satisfied the pore pressure gradient conditions on both Jade and Jade fields and addition to that, find the fracture gradients from the Kirsch's equation (Haimson and Fairhurst, 1970; Zhang and Roegiers, 2010).

Tensile failure method (Kirsch's equation) can be used to find the fracture pressures for both Judy and Jade fields which were verified from Tau model.

$$P_{FP} = \frac{3v}{2(1-v)}(\sigma_v - p) + p \qquad v = 0.3, 0.35 \text{ for shale and chalk (Scribd.com 2013)}$$

4.8.1 Fracture gradients for Judy field:

Depth (ftbsf)	Overburden stress (psi)	Pore pressure (psi)	Fracture gradients (psi/ft)
11056.4	10558.74	8109.77	0.875
11286.0	10747.29	8298.32	0.874
11482.9	10964.85	8515.88	0.878
12237.5	11719.04	9270.07	0.885
12500.0	11980.11	9531.14	0.888
12664.0	12125.15	9676.18	0.888
13057.7	12415.22	9966.25	0.883
13156.1	12574.76	10,125.79	0.889
13484.2	12908.35	10459.38	0.892
13845.1	13198.43	10749.46	0.893
13943.5	13328.96	10879.99	0.893

Table 17. Judy field fracture gradient.
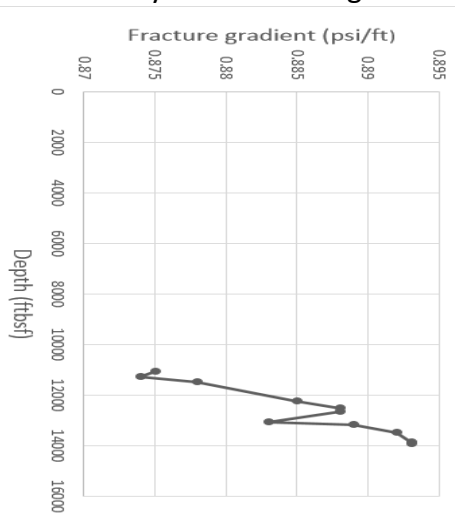
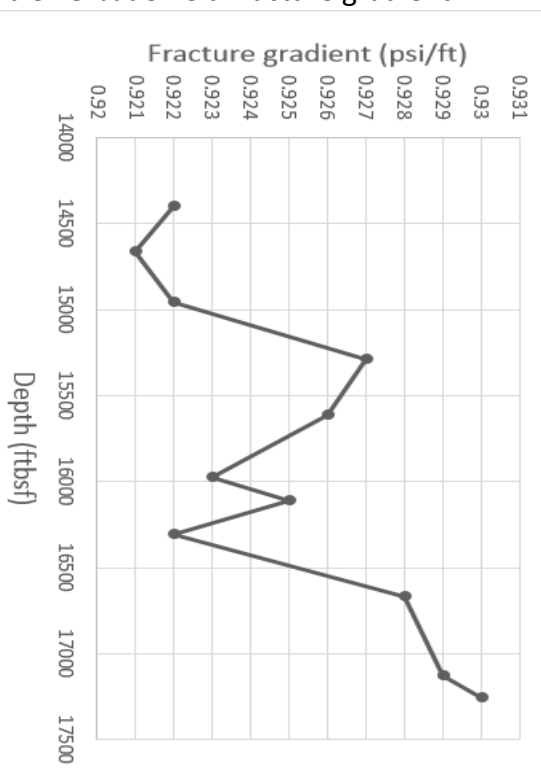Plot 15. Judy field fracture gradient trend line.

Minimum stress method applied on Judy field, this model gave reliable results for Judy field fracture gradient trend line (plot 15). This fracture gradient trend line increased with depth for Judy field. However, the fundamental theory (figure 2) explained, the fracture gradient trend line increased with depth. Thus, the minimum stress method gave correct result for Judy field.

4.8.2 Fracture gradients for Jade field:

Depth (ftbsf)	Overburden stress (psi)	Pore pressure (psi)	Fracture gradients (psi/ft)
14402.8	13764.07	11315.10	0.922
14665.3	13981.63	11532.66	0.921
14960.6	14271.70	11822.73	0.922
15288.7	14648.80	12199.83	0.927
15616.7	14938.88	12489.91	0.926
15977.6	15228.95	12779.98	0.923
16108.9	15373.99	12925.02	0.925
16305.7	15519.03	13070.06	0.922
16666.6	15954.14	13505.17	0.928
17125.9	16389.26	13940.29	0.929
17257.2	16534.29	14085.32	0.930

Table 18. Jade field fracture gradient.

Plot 16. Jade field fracture gradient trend line.

Minimum stress method applied on Jade field, this model gave reliable results for Jade field fracture gradient trend line (plot 16). This fracture gradient trend line increased with depth for Jade field. However, the fundamental theory (figure 2) explained, the fracture gradient trend line increased with depth. Thus, the minimum stress method gave correct result for Jade field.

4.9 ANALYSIS OF PORE, FRACTURE AND OVERBURDEN GRADIENTS RESULTS

4.9.1 Judy field all gradients:

Judy field's pore, fracture and overburden gradient comparison with depth.

Depth (ftbsf)	Pore pressure gradient (psi/ft)	Fracture gradient (psi/ft)	Overburden gradient (psi/ft)
11056.4	0.733	0.875	0.954
11286.0	0.735	0.874	0.952
11482.9	0.741	0.878	0.954
12237.5	0.757	0.885	0.957
12500.0	0.762	0.888	0.958
12664.0	0.764	0.888	0.957
13057.7	0.763	0.883	0.950
13156.1	0.769	0.889	0.955
13484.2	0.775	0.892	0.957
13845.1	0.776	0.893	0.953
13943.5	0.780	0.893	0.955

Table 19. Judy field pore, fracture and overburden gradients.
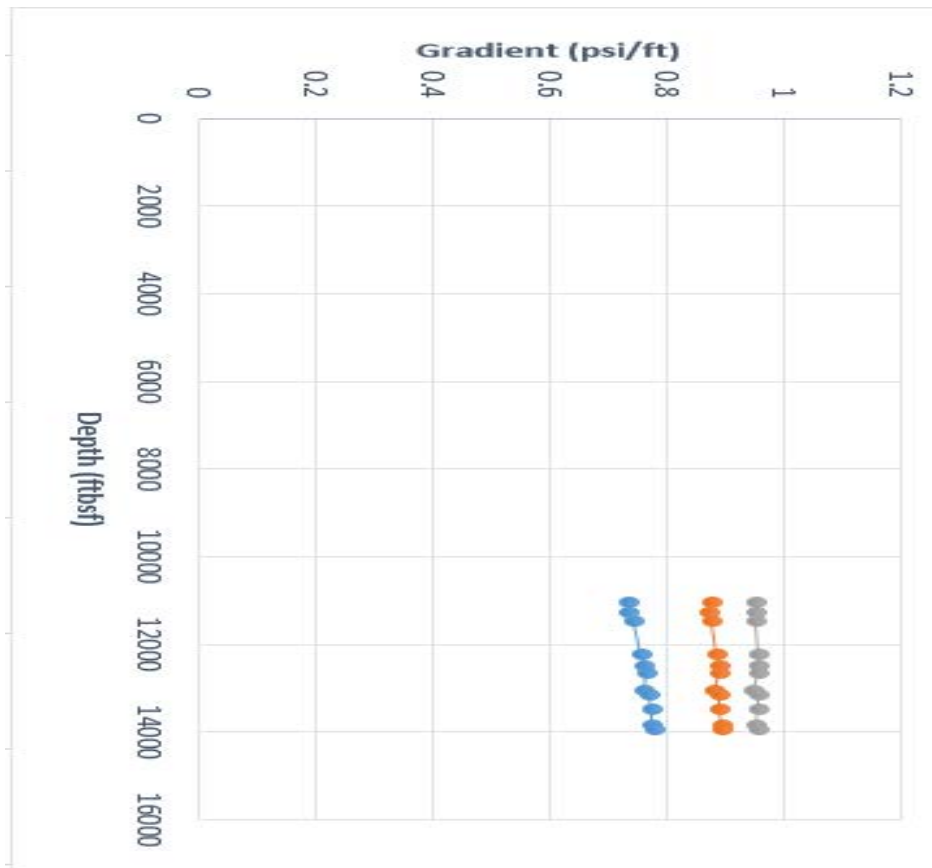
Plot 17: Comparison of pore, fracture and overburden gradients of Judy field.

All pressure gradients such as pore pressure gradient, fracture gradient and overburden pressure gradients compared with depth in the plot 17, this trend lines similar to fundamental theory (figure 2) trend lines. Thus, the chosen models gave correct results and verified on Judy field.

4.9.2 Jade field all gradients:

Jade field's pore, fracture and overburden gradient comparison with depth.

Depth (ftbsf)	Pore pressure gradient (psi/ft)	Fracture gradient (psi/ft)	Overburden gradient (psi/ft)
14402.8	0.785	0.922	0.955
14665.3	0.786	0.921	0.953
14960.6	0.790	0.922	0.953
15288.7	0.797	0.927	0.958
15616.7	0.799	0.926	0.956
15977.6	0.799	0.923	0.953
16108.9	0.802	0.925	0.954
16305.7	0.801	0.922	0.951
16666.6	0.810	0.928	0.957
17125.9	0.813	0.929	0.956
17257.2	0.816	0.930	0.958

Table 20. Jade field pore, fracture and overburden gradients.

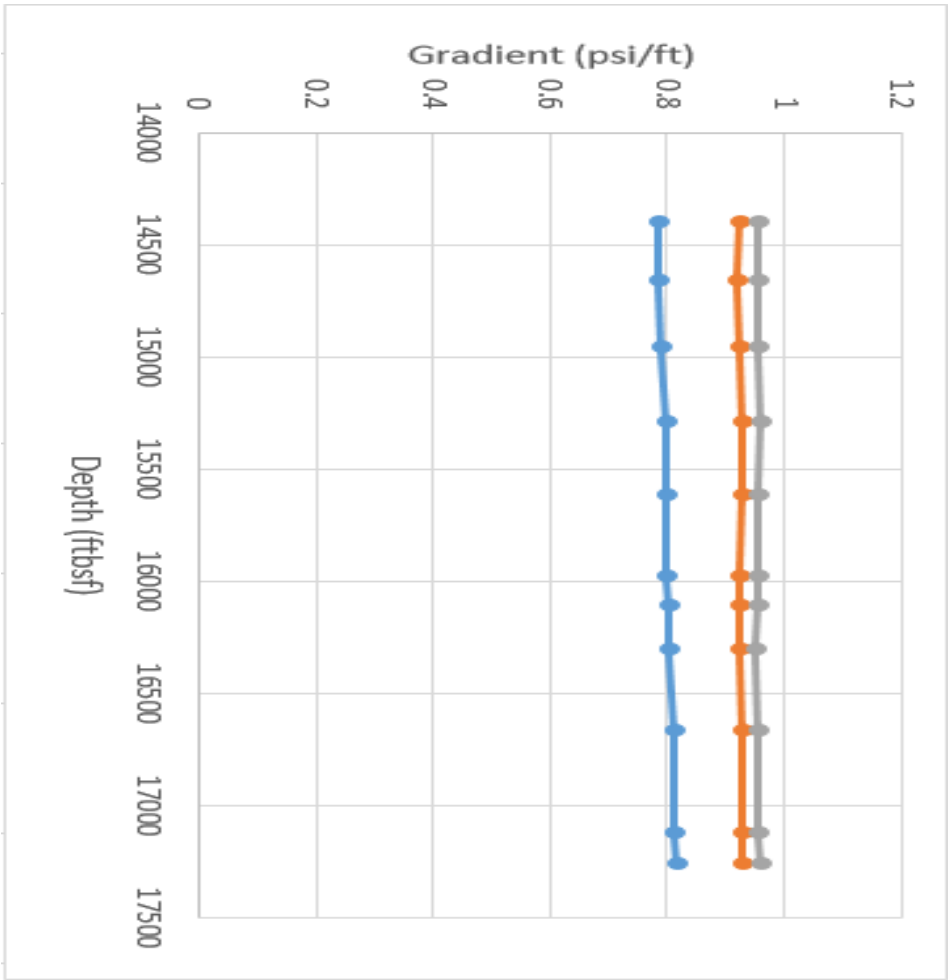Plot 18: Comparison pore, fracture and overburden gradients of Jade field

All pressure gradients such as pore pressure gradient, fracture gradient and overburden pressure gradients compared with depth in the plot 18, this trend lines similar to fundamental theory (figure 2) trend lines. Thus, the chosen models gave correct results and verified on Jade field.

CHAPTER 5

5.0 CONCLUSIONS AND RECOMMENDATIONS

5.1 CONCLUSIONS:

The purpose of this project was to develop a pore pressure and fracture gradient prediction strategy for the Judy and Jade fields in the North Sea Central Graben. The offset well data consisted of Judy and Jade HPHT fields. Multiple pore pressure prediction strategies were reviewed that gave reasonable results: Pore pressure prediction from porosity model and Tau model equations for both porosity and seismic velocity data. Attempts were made to verify the validity of these approaches by comparing the results with pressure depth for sediments. Those attempts gave reasonable results in both fields. However, porosity based pore pressure prediction model does not always deliver a satisfactory pore pressure estimation. There were several reasons for failure to the porosity based method, especially in high temperature basins and higher depths. Pore pressure prediction from porosity model, gave the pore pressure gradients for both Judy and Jade fields were fluctuated and decreased along with depth increased. Tau model gave the good results in both fields, those pore pressure gradients increased along with depths increased. The significant point was the Tau model more appropriate at high depths, because from table 15 and table 16, the pore pressure gradients at high depths similar to available pore pressure gradients, thus the Tau model more suitable to predict the pore pressure gradients at higher depths and overpressured fields. This scenario explained and supported the fundamental lithostatic gradient plot. Therefore, the Tau model was concluded to be the best pore pressure prediction method for future wells in Judy and Jade fields.

The fracture gradient prediction method proposed by Kirsch's solution (tensile failure method) was practical using area precise information and an autonomous foundation for the connection between Poisson's ratio and pore pressure. This method allows fracture gradient prediction and was concluded to be appropriate for future use in these areas.

5.2 RECOMMENDATIONS:

While the above-mentioned pore pressure and fracture gradient prediction methods were allowed for the limited availability and quality of data, there was certain improbability in the precision of the forecasts. The following commendations concerning those uncertainties should be addressed when planning and conducting future drilling operations.

- Porosity based pore pressure prediction method can deliver suitable pore pressure prediction where the overpressure is under compaction and the deposits are young and at low temperatures. Identifying the petroleum systems are both complex and varied, and constantly postulate a series of improbability in pore pressure prediction for future wells.

- Calibration using offset wells, emerging local consideration of wireline and rock characteristics to standardise prediction results. Retaining field modelling seismic and wireline based prediction techniques deliver balancing outcomes and appreciated perceptions into the accurate series of improbability in prediction.

- The best fitting parameters of the Tau model varies from region to region, the assumed fitting parameters to be depends on region lithology. Realistic pore pressures are required to make reliable fracture gradient calculations.

REFERENCES

Ashton, K., Sylte, J.E., Thomas, L.K., and Dixon, T.N. (1998) 'Judy/Joanne Field Development.' [online] available from: < http://www.onepetro.org/mslib/app/Preview.do?paperNumber=00049128&societyCode=SPE> [27-30 Sep. 1998]

Bowers, G.L. (2001) 'Determining an Appropriate Pore-Pressure Estimation Strategy.' [online] available from: < http://www.onepetro.org/mslib/servlet/onepetropreview?id=OTC-13042-MS>[30 April-3 May 2001]

Bowers, G.L. (1995) 'Pore Pressure Estimation from Velocity Data: Accounting for Overpressure Mechanisms besides Undercompaction.' Journal of *SPE Drilling & Completion* 10, 89-95

Burrus, J. (1998) 'Overpressure models for clastic rocks, their relation to hydrocarbon expulsion: a critical reevaluation.' In: Law, B.E., Ulmishek, G.F., Slavin, V.I. (Eds.), Abnormal pressures in hydrostatic environments: AAPG Memoir, 70, pp.35-63

Chatterjee, A., Mondal, S., Basu, P., Patel, B.K., and Reliance Industries Limited (Petroleum E&P). (2012) 'Pore Pressure Prediction Using Seismic Velocities for Deepwater High Temperature- High Pressure Well in Offshore Krishna Godavari Basin, India.' [online] available from: <http://www.onepetro.org/mslib/app/Preview.do?paperNumber=SPE-153764-MS&societyCode=SPE> [28-30 Mar.2012]

Daines, S.R. (1982) 'Prediction of Fracture Pressures for Wildcat Wells.' [online] available from: <http://www.onepetro.org/mslib/servlet/onepetropreview?id=00009254>[April 1982]

Daniel, R.B. (2001) 'Pressure prediction for a Central Graben wildcat well, UK North Sea.' *Marine and Petroleum Geology*, 18, 235-250

Dickinson, G. (1951) 'Geological Aspects of Abnormal Reservoir Pressures in the Gulf Coast Region of Louisiana, U.S.A.' [online] available from: <http://www.onepetro.org/mslib/servlet/onepetropreview?id=WPC-4001>[May 28 - June 6, 1951]

Dutta, N.C. (2002) 'Geopressure prediction using seismic data: Current status and the road ahead.' *Geophysics*, 67, 2012-2041

Eaton, B.A. (1968) 'Fracture Gradient Prediction and Its Application in Oilfield Operations.' *Petroleum Technology*, 21, 1353-1360

Eaton, B.A. (1972) 'The Effect of Overburden Stress on Geopressure Prediction from Well Logs.' *Petroleum Technology*, 24, 929-934

Eaton, B.A. (1975) 'The Equation for Geopressure Prediction from Well Logs.' [online] available from: < http://www.onepetro.org/mslib/servlet/onepetropreview?id=00005544>[September-1 October 1975]

Flemings, P.B., Stump, B.B., Finkbeiner, T., Zoback, M. (2002) 'Flow focusing in overpressured sandstones: theory, observations, and applications. Am. J. Sci.302, 827-855

Fooshee, J.S. (2009) 'The development of a pore pressure and fracture gradient prediction model for the Ewing banks 910 area in THE Gulf of Mexico.' [online] available from: <http://etd.lsu.edu/docs/available/etd-01202009-143411/> [20 Jan. 2009]

Gardner, G.H.F., Gardner, L.W., Gregory, A.R. (1974) 'Formation velocity and density-the diagnostic basis for stratigraphic traps.' *Geophysics*, 39, 2085-2095

Gutierrez, M.A., Braunsdor, N.R., and Couzens, B.A. (2006) 'Calibration and ranking of pore-pressure prediction models.' *The Leading Edge*, 25, 1516–1523

Haimson, B.C., Fairhurst, C. (1970) 'In situ stress determination at great depth by means of hydraulic fracturing.' In: Somerton, W.H. (Ed.), Rock Mechanics-theory and practice. Am. Inst. Mining. Eng., pp. 559-584

Hawkins, K., Ratcliffe, A., Roberts, G., Went, D. and DGC, V. (2004) High Resolution Pore-pressure Prediction from AVO Derived Velocities; a North Sea Case Study [online] available from <http://www.onepetro.org/mslib/servlet/onepetropreview?id=SEG-2004-0366>

Heppard, P.D., Cander, H.S., Eggertson, E.B. (1998) 'Abnormal pressure and the occurrence of hydrocarbons in offshore eastern Trinidad, West Indies.' In: Law, B.E., Ulmishek, G.F., Slavin, V.I. (Eds.), Abnormal Pressures in Hydrocarbon Environments: AAPG Memoir, 70, pp. 215-246

Holbrook,P.W., Maggiori, D.A. (1995) 'Real-Time Pore Pressure and Fracture Gradient Evaluation in All Sedimentary Lithologies.' *SPE Formation Evaluation*, 10, 215-222

Hottmann, C.E., Johnson, R.K. (1965) 'Estimation of Formation Pressures from Log-Derived Shale Properties.' *Petroleum Technology*, 17, 717-722

Law, B.E., Spencer, C.W. (1998) 'Abnormal pressures in hydrocarbon environments.' In: Law, B.E., Ulmishek, G.F., Slavin, V.I. (Eds.), Abnormal Pressures in Hydrocarbon Environments: AAPG Memoir, 70, pp. 1-11

Morley, C.K., King, R., Hillis, R., Tingay, M., Backe, G. (2011) 'Deepwater fold and thrust belt classification, tectonics, structure and hydrocarbon prospectivity: A review.' *Earth-Science Review*, 104, 41-91

Mouchet, J.C., Mitchell, A. (1989) 'Abnormal Pressure while Drilling.' Editions TECHINIP, Paris

Nelson, H.N., Bird, K.J. (2005) 'Porosity-Depth Trends and Regional Uplift Calculated from Sonic Logs, National Reserves in Alaska.' Scientific Investigation Report 2005-5051 U.S. Dept. of the Interior and USGS

Nguyen, T.T.B; Jones, J.S; Goulty, N.R; Middleton, A.J; Grant, N; Ferguson, A; Bowen, L. (2013) 'The role of fluid pressure and diagenetic cements for porosity preservation in Triassic fluvial reservoirs of the Central Graben, North Sea.' *the American Association of Petroleum Geologists*, 97, 1273-1302

Nygaard, R., Karimi, M., Hareland, G., Tahmeen, M., and Munro, H. (2008) 'Pore Pressure Prediction in Overconsolidated Shales.' [online] available from: < http://www.onepetro.org/mslib/app/Preview.do?paperNumber=SPE-116619-MS&societyCode=SPE>[11-15 Oct. 2008]

Ovens, J., Charles, R. (2010) 'Jade field: Late - life development challenges in a Triassic HPHT gas condensate reservoir.' [online] available from : < http://petex.pesgb.org.uk/cgi-bin/somsid.cgi?page=html/abstracts/abstractid49> [18 Aug. 2013]

Offshore technology (2012) 'Jasmine Field, North Sea, United Kingdom.' [online] available from: < http://www.offshore-technology.com/projects/jasminefieldnorthsea/> [18 Aug.2013]

Powley, D.E. (1990) 'Pressures and hydrogeology in petroleum basins.' *Earth-Science Reviews*, 29, 215-226

Primio, R. D., Neumann, V. (2008) 'HPHT reservoir evolution*: a* case study *from* Jade *and* Judy fields*,* Central Graben*,* UK North Sea.*' Earth Sciences*, 97*,* 1101-1114

*Sborne, M.J., Swarbrick, R.E. (1999) '*Diagenesis in North Sea HPHT clastic reservoirs — consequences for porosity and overpressure prediction.' *Marine and Petroleum Geology*, 16, 337-353

Sayers, C.M., Johnson, G.M., Schlumberger., Denyer, G., and EEX Corporation. (2000) 'Predrill Pore Pressure Prediction Using Seismic Data.' [online] available from : < http://www.onepetro.org/mslib/servlet/onepetropreview?id=00059122> [23-25 Feb. 2000]

Swarbrick, R.E., Osborne, M.J., Grunberger, D., Yardley, G.S., Macleod, G., Aplin, A.C., Larter, S.R., Knight. V. and Auld, H.A. (2000) 'Integrated study of the Judy Field (Block 30/7a) — an overpressured Central North Sea oil/gas field'. *Marine and Petroleum Geology*, 17, 993–1010

Swarbrick, R.E. (2001) 'Challenges of porosity – based pore pressure prediction.' [online] available from:
<http://www.earthdoc.org/publication/publicationdetails/?publication=4437>

Swarbrick, R. (2012) 'Review of pore-pressure prediction challenges in high-temperature areas'. *The Society of Exploration Geophysicists*, 31, 1288-1294

Swarbrick, R.E., Osborne, M.J. (1998) 'Mechanisms that generate abnormal pressures: an overview. In: Law, B.E., Ulmishek, G.F., Slavin, V.I. (Eds.), Pressure Regimes in Sedimentary Basins and their Prediction: AAPG Memoir, 70, pp. 13-34

Swarbrick, R.E., Osborne, M.J., Yardley, G.S. (2002) 'Comparison of overpressure magnitude resulting from the main generating mechanisms. In: Huffman, A.R., Bowers, G.L. (Eds.), Pressure Regimes in Sedimentary Basins and their Prediction: AAPG Memoir, 76, pp. 1-12

Ward, C.D., Sperry-Sun Drilling Services; Coghill, K., BP Norge U.A.; Broussard, M.D., and Amoco Norway Oil Company. (1994) 'The Application of Petrophysical Data to Improve Pore and Fracture Pressure Determination in North Sea Central Graben HPHT Wells.' [online] available from:<
http://www.onepetro.org/mslib/app/Preview.do?paperNumber=00028297&societyCode=S PE>[25-28 Sep.1994]

Winthaegen, P.L.A., Verweij, J.M. (2003) 'Estimating regional pore pressure distribution using 3D seismicvelocities in the Dutch Central North Sea Graben.' *Geochemical Exploration*, 78-79, 203–207

Yardley, G.S., Swarbrick, R.E. (2000) 'Lateral transfer: a source of additional overpressure?.' *Marine and Petroleum Geology*, 17, 523-537

Zhang, J. (2011) 'Pore pressure prediction from well logs: Methods, modifications, and new approaches.' *Earth-Science Reviews*, 108, 50–63